Reviews

Modular design of icosahedral metal clusters

N. A. Bulienkov and D. L. Tytik*

Institute of Physical Chemistry, Russian Academy of Sciences,
31 Leninsky prosp., 117915 Moscow, Russian Federation.
Fax: +7 (095) 952 5308. E-mail: lmm@serv1.phyche.ac.ru

The concept of crystalline "module," that is, an unambiguously isolated, repeated quasi-molecular element, is introduced. This concept is more general than the concept of crystal lattice. The generalized modular approach allows extension of the methods and principles of crystallography to quasi-crystals, clusters, amorphous solids, and periodic biological structures. Principles of construction of aperiodic, nonequilibrium regular modular structures are formulated. Limitations on the size of icosahedral clusters are due to the presence of spherical shells with non-Euclidean tetrahedral tiling in their structure. A parametric relationship between the structures of icosahedral fullerenes and metal clusters of the Chini series was found.

Key words: crystalline module, local order, "internal" coordinates, parametric structures, algorithm, icosahedral clusters, quasi-crystals, fullerenes.

Introduction

Ideas of interdisciplinary investigation of the processes of self-organization of matter on the atom-molecular level penetrate more and more deeply into new technologies of creating materials with stable structure under nonequilibrium conditions.

Until recently, crystalline substances and natural materials, as well as man-made materials obtained under nearly equilibrium conditions, have mostly been studied. Diffraction methods were developed on the basis of the concept "lattice"; they were efficient in studying crystal structures including biocrystals and made it possible to obtain reliable stereochemical and crystal chemistry data. However, advances in the use of diffraction methods for studying the crystal structure were to a certain extent a cause of erosion of interest in studies of self-organization processes, which seemed to be self-evident for crystalline solids.

Advances of diffraction methods in studying aperiodic and amorphous structures appeared to be much more conservative, since there were no concepts for adequate description of the structure of these substances. Creation of new methods for investigation of aperiodic and amorphous structures requires new ideas, which could play the role of the concept "crystal lattice," which is the basic concept of classical crystallography. A necessary step in this direction is such a generalization of crystallography that could cover all known non-crystalline forms of solids. Frequent use of such concepts as "design," "engineering," "constructing," "architecture," and "ensemble" reflects the essential role of geometry for stereochemistry and crystal chemistry in constructing model structures. The priority of the theoretical approach fully corresponds to the evident trend to use the potentialities of structural self-organization of substances on the molecular level for targeted control in creating those materials which cannot be obtained by natural means or are unknown as yet.

Published in Russian in *Izvestiya Akademii Nauk. Seriya Khimicheskaya,* No. 1, pp. 1—19, January, 2001.

1066-5285/00/5001-0001 $25.00

Among aperiodic quasi-molecular structures, a special place is occupied by metal clusters, which are promising objects of investigation, since they have a simple composition and possess well-studied properties. They can be used as monodisperse particles in nanotechnologies of highly organized materials with hierarchic structure.

One of the most important tasks in creating advanced materials with unique quantum-size properties is to synthesize monodisperse ligand-free ("naked") metal clusters considered as basic "building blocks" and to establish their structure. Knowledge of nonequilibrium structures of the clusters will allow deliberate selection of stabilizing ligands and formation of precursor materials that can be organized to form regular structures under the action of molecular forces. As a result, this will make it possible to produce such alloys that cannot be obtained by conventional high-temperature "metallurgical" methods.

Apart from their mesomorphous structure, which is intermediate between the molecular and crystal structure, the ligand-free metal clusters are essentially nonequilibrium structures characterized by high density of states of the "energy landscape".[1] For metastable structures, the most important is to attain a maximum stability due to the formation of numerous nearly undistorted bonds rather than the position of the potential energy minimum. Because of the absence of translational symmetry in clusters and their small size (at most 1 μm) no effective diffraction methods for studying the cluster structure are available.[2—4] The same problems are also characteristic of the material science of nanocomposites and quasi-crystals (nanocomposites self-organized from clusters).[5] In this connection, the main method of investigation of the cluster structure is modeling based on indirect experimental data obtained by different methods, taking into account the peculiarities of the AO structure and the results of semiempirical quantum-mechanical calculations.[6]

Despite their aperiodic structure, the ligand-free clusters retain some features of the crystal structure inherent in the cluster matter in the equilibrium state. These features are associated with local order and simplicial-modular tilings* entirely along chemical bonds, which characterize geometric parameters of their total jointing and, hence, the structure stability. Simplicial[7] and modular[8] tilings of crystal structures are unambiguous; however, the rules of jointing of the modules in the noncrystalline structures can be different and can disturb periodicity, though retaining local similarity to the crystal structure. The parameters of simplicial-modular tilings in any structure are "internal" coordinates of chemical bonds (the bond length, d; the bond angle, Ψ; and the torsion angle of bond twist, θ),[9] which reflect the bond stereochemistry. Therefore, by retaining the total jointing of bonds in modular models of the structure and by estimating the changes in the internal parameters of the bonds in aperiodic structures it is possible to choose the most appropriate (from symmetry considerations) variant from several feasible variants. Among important criteria for such a choice are the results of mass spectrometric studies, as well as data on the ionization potentials and melting temperatures,[10—12] which allow determination of the number of atoms in stable clusters. In contrast to conventional methods of structure modeling, modular design based on a system of concepts, principles, and algorithms uses no quantum-mechanical or approximate band energy calculations.

The aim of this review is to study the potentialities of modular design in creating cluster structures. We have to begin with the design of a particular kind of metal clusters with known structural models that are in agreement with experimental data. Icosahedral metal clusters are best suited to this purpose.[13] Correspondence between the known structures of these clusters and the models obtained by the method of modular design will allow one to elucidate the potentialities of this method. Only upon completing this work can modular design be applied to other types of metal clusters with unknown structural models.

Simplicial-modular tiling of the crystal close packings and their local order

An invariant of the structure of a metal cluster, which is also the same for the equilibrium crystal structure of the metal, is characterized by a fragment of the crystal structure inscribed in a sphere of radius no greater than two shortest interatomic distances. The long-range order, which is due to periodicity, is only formally described by the crystal lattice, since physicochemical and geometric conditions for the lattice formation are not evident. In a crystal structure, the structural fragment completely determining the long-range order is inscribed in a sphere of radius from two to four interatomic distances, depending on the structure complexity.[14] Therefore, the design of aperiodic cluster structures requires the use of (i) the polyhedra of simplicial-modular tilings of relevant crystal structures and (ii) such binary symmetry operations for jointing the polyhedra (*e.g.*, twinning) that are absent in the space group of the crystal and, hence, disturb periodicity.

Simplicial tiling and local order in the crystal packings of equal spheres. There are two types of the crystal close packings in metal structures, namely, the face-centered cubic (fcc) packing and the hexagonal close packing (hcp). Total jointing of bonds and maximum density are conditions for the structure stability of any solid. In any structure, it is possible to isolate polyhedral simplices in such a way that their vertices are occupied by atoms and

* A simplex is a polyhedron formed by the atoms of the structure, which lie on the surface of an empty sphere; the edges of this polyhedron are the shortest interatomic distances (chemical bonds). A module is a void in the crystal structure, which is unambiguously isolated only by chemical bonds. The modules are parallelohedra formed by several simplices and continuously fill the whole space by translations.

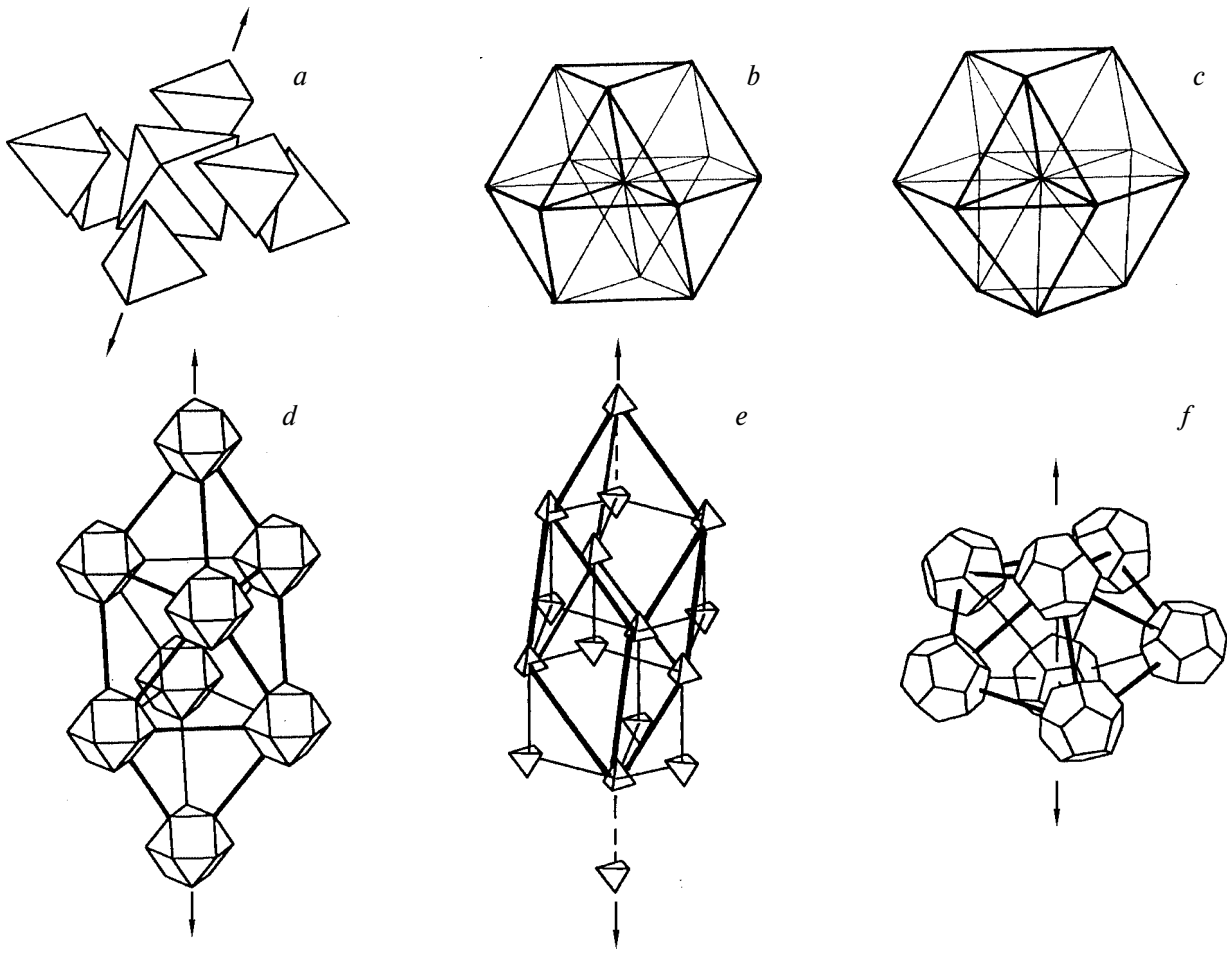

Fig. 1. Simplicial-modular tiling of two layers of the fcc and hexagonal close packings of spheres: tetrahedral and octahedral simplices and the R-module consisting of two tetrahedra and one octahedron (the C_3 axis is shown by arrows) (*a*); the first coordination sphere of the fcc (*b*) and hexagonal close (*c*) packings responsible for the local order; "internal" parameters of the bonds in crystalline modules of the fcc structure (*m*, $\theta = 0°$) (*d*), diamond ($\bar{1}$, $\theta = 60°$) (*e*), and in the D_{5h}-module of the {3,3,5} polytope (*m*, $\theta = 0°$) (*f*).

their edges are chemical bonds (the shortest interatomic distances). In the close crystal packings of spheres, these simplices are represented by two types of hollows, *viz.*, regular tetrahedra (tetrahedral sites) and regular octahedra (octahedral sites) with the edge lengths equal to the length of the chemical bond and with triangular faces.[15] Three such simplices (two tetrahedra and one octahedron) can be united to form a parallelohedron, or a module (here, a regular rhombohedron) with no atoms inside and chemical bonds as edges (Fig. 1, *a*). In the fcc packing, the rhombohedral R-module* is simultaneously the rhombohedral unit cell built on the shortest 1/2 ⟨110⟩ translations. The whole crystalline space of the fcc and hexagonal close packings can be continuously filled with such modules.

To determine the local order in simple (fcc and hcp) crystal structures, it is sufficient to use a part of the first coordination sphere, namely, a Delone star comprised of eight tetrahedra and six semioctahedra (stereohedra of octahedral simplex) (see Fig. 1, *b*, *c*). In the fcc structure, simplices of the same type are united only by sharing vertices and edges, whereas in the hcp structure they can also share one of the faces, thus forming continuous columns of octahedra and tetrahedra along a C_3 axis.[15]

As was mentioned above, description of simplicial-modular polyhedra requires the use of "internal" coordinates, which have both geometric and energy meaning.[9] This makes it possible to reveal binary symmetry operations ($\bar{1}$, *m*, 2) responsible for total jointing of all bonds between the atoms in simplices and modules and, hence, in relevant structures, thus ensuring their stability. In the fcc structure with cuboctahedral coordination, all bonds are oriented along the ⟨110⟩ direction and therefore all atoms can be replaced by a bundle of twelve ⟨110⟩ directions issuing out of all the cuboctahedron vertices. Analogously, in the diamond structure, all rays in the

* Hereafter, the notations of the modules and simplices are given using either their point symmetry groups or morphology.

bundle issue out of all the tetrahedron vertices, while in the icosahedral structure of the {3,3,5} polytope they issue out of all the pentagondodecahedron vertices of a four-dimensional icosahedron comprised of interpenetrating icosahedra.[16] Such "polyhedral" atoms in the modules of these structures are jointed by the bonds issuing out of vertices or by the normals to their faces using binary symmetry operations m (symmetry plane) and parameter $\theta = 0°$ in the fcc structure, $\bar{1}$ (center of symmetry) and parameter $\theta = 60°$ in the diamond structure, and m and parameter $\theta = 0°$ in the D_{5h}-module of the {3,3,5} polytope (see Fig. 1, *d*—*f*, respectively).

In icosahedral and tetrahedral structures and two-dimensional pentagonal mosaics, the binary symmetry operations used for joining of (i) the atoms in simplices and (ii) the simplices in modules are self-similar. As can be seen in Fig. 1, *f*, five tetrahedral simplices in the D_{5h}-module of the {3,3,5} polytope are also joined by sharing faces using the binary symmetry operation m.[16]

Crystalline parallelohedral modules and their properties. A crystalline module considered as a quasi-molecule corresponds to Fedorov's "crystalline molecule,"[17] which differs from conventional chemical molecules. In contrast to the crystal lattice, a crystalline module is unambiguously isolated in the structure[8] by using the Belov structural motif in the polyhedral representation, which is the basis of the crystal-chemical classification.[15] Atoms in the module can be located not only at vertices, but also on the edges and faces, so that they are bound with one another by real chemical bonds to form a rigid framework. The parallelohedral shape of modules predetermines continuous filling of the crystalline space despite the fact that modules are most often not the unit cells of the crystal lattice. The module contains information on the long-range order up to the macrocrystal morphology determined by the most important faces. Consider the diamond module (see Fig. 1, *e*) corresponding to the carbon cage of the diadamantane molecule, $C_{14}H_{20}$. Here, the two-dimensional modular loops, namely, hexacycles with a "chair" conformation ($\bar{1}$, $\theta = 60°$), determine the structure of octahedral faces, which are the most important faces in the morphology of diamond. The normals to three "outer" pairs of parallel hexacycles and to the fourth ("equatorial") hexacycle of the diamond module coincide with the normals to the octahedral faces. The point group of the diamond module ($G^3_{0(M)}$—$\bar{3}m$) is the subgroup of the point group of diamond crystal ($G_0{}^3$—$m\bar{3}m$). Taking into account the jointing of the vertices, edges, and faces of modules in the crystal structure, the compositions of the modules correspond to stoichiometry. Therefore, the local and global compositions correspond to stoichiometry only in crystals built up from modules of the same type.[8,16] Self-organization of the crystal structure of diamond is completely determined by the only parameter ($\theta = 60°$) prescribed for each bond.

The elementary act of crystal growth involves the closure of two-dimensional modular loops in atomic nets of the faces with maximum reticular density and completion of three-dimensional modules in the tangential growth layer of thickness one module. Modular design is used in the case of chemical compounds containing several kinds of atoms. Metal clusters with the fcc and hcp structures can be designed using both modules and simplices.

The module of the NaCl structure (Fig. 2, *a*)[8] is a cube with the edge equal to half the lattice constant. The cube vertices are occupied by Na and Cl atoms located at tetrahedral positions. Formally, this cube can be divided into five tetrahedral simplices (one regular simplex at the cube center and four irregular simplices such that each of them shares one vertex with the vertices of the cube module). However, the (Na—Na) edges, which are not chemical bonds, appear in such simplices, which contradicts the accepted conditions necessary for maximum stability. In fact, two- and three-dimensional modular loops (see Fig. 2, *b*, *c*) were used in the models of the $[(NaCl)_m(Na)_2]^{2+}$ (m = 11 and 12) clusters. The notations of these clusters ($5 \cdot 3 \cdot 1 + 3 \cdot 3 \cdot 1$) give the number of atoms in the orthogonal arrays of two two-dimensional atomic nets[18] and can be replaced by the number of edges of modular loops in these nets ($4 \cdot 2 + 2 \cdot 2$).

Transformation of crystalline modules into non-Euclidean modules of regular structures of curved spaces of constant curvature. Crystalline modules can be cooperatively transformed without appreciable changes in the bond lengths and bond angles into non-Euclidean modules of regular structures of curved spaces with opposite signs of curvature. However, continuous filling of the

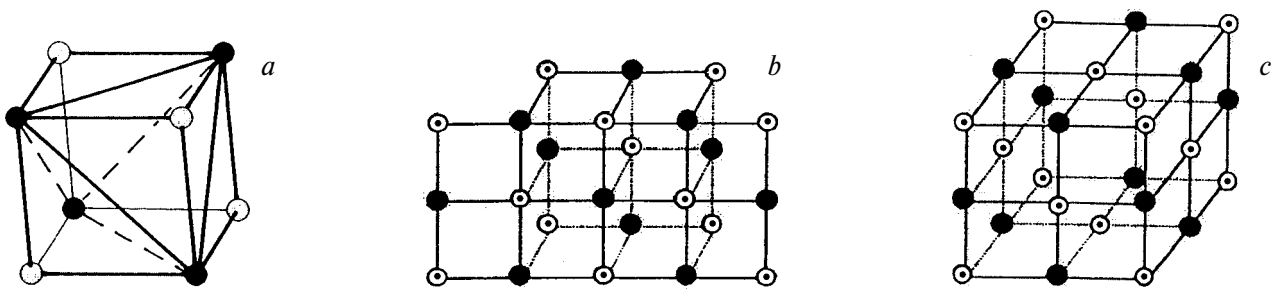

Fig. 2. Module of NaCl structure (*a*); two- and three-dimensional modules of NaCl structure in the model of charged cluster $[(NaCl)_mNa_2]^{2+}$: m = 11 ($5\times3\times1 + 3\times3\times1$) or ($4\times2 + 2\times2$) (*b*) and m = 12 ($3\times3\times3 - 1$) or ($2\times2\times2$) with point defect V°_{Cl} (*c*).[18]

three-dimensional Euclidean space (so natural for any atomic structure with real chemical bonds whose lengths can vary only within particular limits!) by the transformed modules is ruled out because of the disclination* components of these transformations.[16,19]

Crystalline modules continuously fill the Euclidean space by translations. Owing to their Euclidean nature, no strain occurs in the structure in the case of ideal crystal growth; therefore, the crystalline modules correspond to equilibrium states, and an energy equal to the heat of melting is released upon the formation of crystals. The transformed non-Euclidean modules can be only locally embedded in the Euclidean space (within a sphere of radius no greater than two to three interatomic distances, depending on the structure type). This restriction is due to the fact that the sum of the angles of a triangle in the spherical and hyperbolic spaces of constant curvature differs from 180° and, what is the most important, by the fact that the difference $\delta = |\alpha + \beta + \gamma| - 180°$ changes with distance from the initial point of growth. Therefore, a growth of the structures formed by non-Euclidean modules inevitably results in an increase in strain, which restricts their size. Unlike crystals, such structures take up energy from the outside upon their formation.

Consider the disclination transformation of the R-module, which is equivalent to the R-lattice (Fig. 3, *a*) of the fcc structure. Let us divide all six faces of this module by short diagonals into equilateral triangles. By removing and inserting the same triangles using the "cut—paste" topological operation, these modules can be cooperatively transformed into non-Euclidean modules of regular structures with a constant curvature: the {3,3,5} polytope in the three-dimensional spherical space S^3 (D_{5h}-module in Fig. 3, *b*, *e*) and a crystalloid in the three-dimensional hyperbolic space H^3 (C_{2v}-module in Fig. 3, *e*).[16] As can be seen in Fig. 3, *c* and *e*, these modules are non-Euclidean, since they are formed using only regular tetrahedral simplices joined by faces. Using similar disclination transformations of the initial Euclidean R-module, it is possible to obtain Bernal′s polyhedra or the so-called "canonical holes" (see Fig. 3, *f*—*h*),[16] which form a random close packing of equal spheres with a constant density at particular ratios.[20] The fcc modules (derivatives of the R-module) of two diamond-

* A disclination is a structural defect, which causes curvature of the planar layer due to the introduction or removal of the layer segment with angle equal to the elementary angle of the symmetry axis.

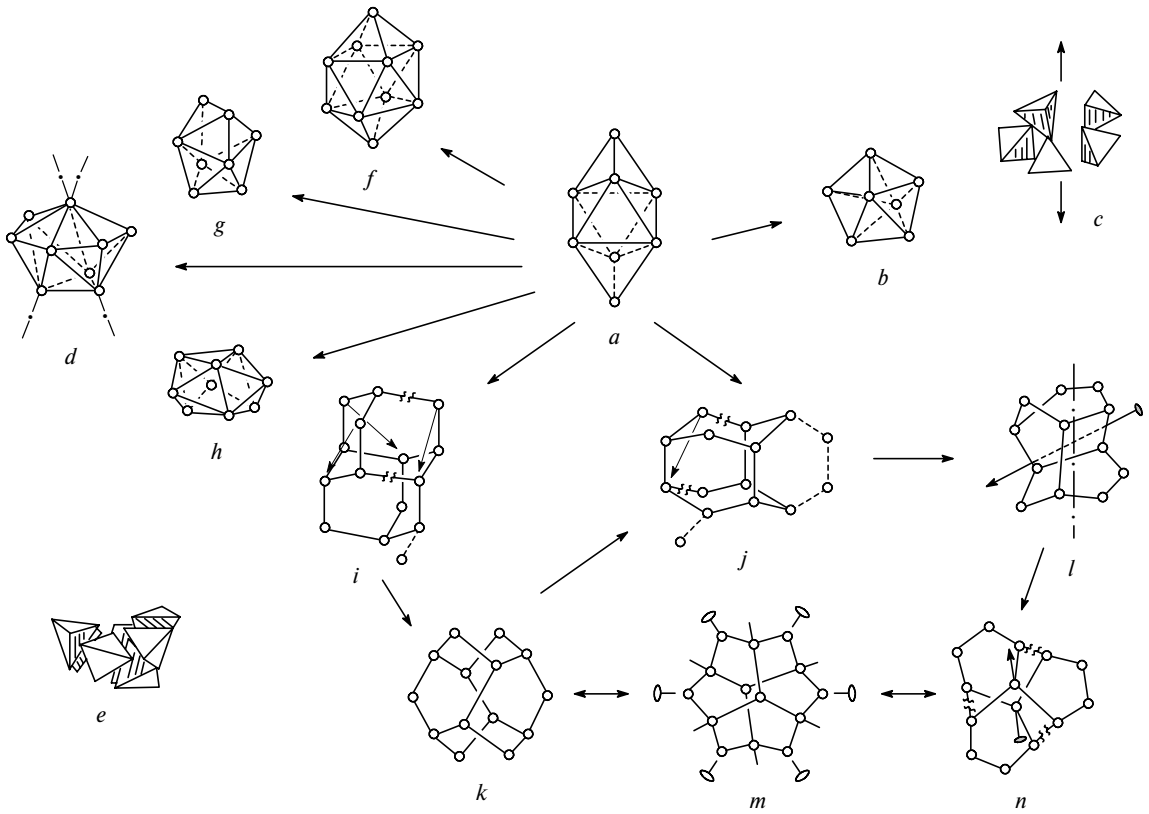

Fig. 3. Channellized system of Euclidean crystalline modules (*a*, *i*, *j*) and transformed non-Euclidean modules[16]: R-module of the fcc lattice (*a*); D_{5h}-module of the {3,3,5} polytope (*b*), and its tiling only into tetrahedral simplices (*c*); C_{2v}-module of crystalloid in the H^3:*P*222 space (*d*) and its tiling into tetrahedral simplices (*e*); Bernal′s "canonical holes," *i.e.*, modules of the random close packing of equal spheres of constant density (*f*—*h*);[20] crystalline modules of diamond (*i*) and ice I*H* (*j*); and transformed non-Euclidean modules (*k*—*n*).

like structures, namely, diamond (a 14-atom M_s-module with D_{3d} symmetry) and ice IH (a 12-atom M_w-module with D_{3h} symmetry), can also be cooperatively transformed into the corresponding non-Euclidean 14-atom K-module with D_2 symmetry and 12-atom H-module with C_2 symmetry.[16,19] All modules form a channellized system in which they are related by mutual cooperative transformations at fixed values of the parameter θ;[16] some of the modules are shown in Fig. 3, *a*—*n*.

Generalized modular crystallography and system-forming hierarchic structures. J. D. Bernal and A. L. Mackay[9,21,22] posed the problem of such a generalization of crystallography that would allow its use in the area of investigation of aperiodic structures including hierarchic structures. This has been made possible on the basis of a new concept of the "crystalline module," which is more general than the concept of the "crystal lattice" but consistently related to it. Generalized crystallography uses a metric based on the "golden section,"* which is the most important condition for the formation of self-similar, hierarchic system-forming structures.[16] It has been possible to introduce such a metric by endowing the points (atoms)** of the structure with the corresponding point symmetry groups, taking into account the directions of lines (bonds) connecting these points in the structure. Only three point symmetry groups suitable for realization of the "golden-section"-based metric exist. These are two three-dimensional groups (T-23 and I_h-$m\bar{3}\bar{5}$) and one two-dimensional group (C_{5v}-5m). The non-Euclidean modules with tetrahedral and icosahedral symmetry of atoms, obtained by cooperative transformations of the R-module of the fcc structure and the M_s- and M_w-modules of diamond-like crystal structures, can be only locally embedded in the three-dimensional Euclidean space and only fractally (discontinuously) translated along determinate directions using binary symmetry operations (m, 2).[16,23,24]

The tetrahedral, self-similar determinate system-forming modular structures of generalized crystallography can form the structures of bound water in biological systems. The "golden-section"-based metric of these structures explicitly predetermined the "metric" selection of a small number of monomers in the main chains of periodic biopolymers (four) and minerals (three) in natural biomineral nanocomposites.[25] The system-forming fractal parametric structures of bound water reflect their predisposition to the forming of biological systems due to the formation of numerous weak hydrogen bonds between the commensurate spatial structures of water and biopolymers, which mutually stabilize one another.[26] It is the absence of a common system-forming component (structures of bound water) and "metric" selection of commensurate components that are responsible for the impossibility of creating such complex hierarchic systems as those known in biology by the methods of supramolecular chemistry despite a great variety of molecular ensembles.[27]

The simplicial-modular tiling of the crystal close packings in combination with binary symmetry operations used for assembling of regular aperiodic modular structures serve as the theoretical basis for the determinate modular design. This method has been proved in the studies of the structure of quasi-crystals,[16] hierarchic system-forming structures of bound water,[16,23—26] hierarchic mosaics,[16] biomineral nanocomposites (bone tissue),[5] amorphous polymodular structures (α-Al_2O_3),[28] and soliton-like configurational defects in perfect crystals of diamond and cadmium sulfide.[29,30]

Principles of modular design and parameters of the algorithms of the structures of icosahedral clusters

Schmid[31] proves the existence of passage from three-dimensional crystal structure to the cluster state and then to monomolecular complexes by the existence of two- and three-dimensional closed modular loops common to all these states. Such loops (in particular, planar hexacycles) are characteristic of the structure of (i) layers of crystalline graphite, (ii) clusters similar to fullerene C_{60}, and (iii) phenanthrene molecules. Another type of two-dimensional modular loops (hexacycles with a "chair" conformation) is an invariant common to the structures of diamond, adamantane, and diadamantane (the carbon cage geometry of this molecule coincides with that of the crystalline module of diamond) (see Fig. 1, *e*), and cyclohexane.[8,16] This confirms justifiability of assembling the cluster structures from blocks (polyhedra of simplices and structural modules) following strictly specified rules.

Principles of modular design of determinate self-organizing cluster structures. Some additional arguments should be advanced in favor of the determinate character of modular cluster structures. First, the modules are a universal form of self-organization of all known forms of solids such as crystals,[8] amorphous solids,[19,28] quasi-crystals,[16,32] fractals,[16,24] and molecular biological systems in the native hydrated state[23—26,33] and it seems likely that clusters are also no exception. Second, both stable values of "magic" numbers characteristic of the cluster structure, found by different methods, and general formulas for calculating possible values of such numbers for the clusters with the same morphology[34,35] suggest that there is a determinate and evolutionary self-assembly of clusters. From this it follows that one of the principles of modular design should be the rule according to which the structure of the preceding "homologue" of the cluster series, corresponding to the series of magic numbers, should serve as a "seed" of

* This metric allows raising the irrational number $\tau = 1.618...$ to the power n by adding and multiplying this number and the integers of the Fibonacci series F_n (0; 1; 1; 2; 3; 5; 8; 13; 21...) following the rule $\tau^n = F_n\tau + F_{n-1}$ provided that $\tau^n = \tau^{n-1} + \tau^{n-2}$ and $F_n = F_{n-1} + F_{n-2}$.

** It should be remembered that a point is the main element in the Euclidean geometry.[17]

the structure of the succeeding "homologue." However, the maxima on the mass spectrogram corresponding to the magic numbers of the atoms of the most stable cluster structures can be assigned not only to the major trunk of the evolutionary tree of clusters, but also to its branches. The aim of the modular design is not only to create the structures of stable clusters, but also to locate the branching points on the evolutionary tree as well as to establish the structures of the clusters corresponding to these branching points. Therefore, of interest is the whole series of clusters and its evolution rather than a particular cluster with a particular magic number value.

Yet another important principle of modular design is the principle of systemic self-organization also known as the "all-or-none" principle.[36] According to this principle, (i) experimental values of all magic numbers for a given type of clusters must be equal to the numbers of atoms for the whole series of modular cluster structures and (ii) particular coincidence of the experimental values of magic numbers with the number of atoms in models is unacceptable.

The principle of modular design itself also corresponds to the determinate structure of clusters. In conventional modeling, attachment of an atom to different structural positions is followed by calculating and comparing the potential energy values in order to determine the most favorable position. In modular design, the sites for adding the atoms are chosen so that the number of newly attached atoms required for the closure of modular loops is minimum. Formally, this process can be represented as jointing of modular or simplicial polyhedra by shared faces, edges, or vertices.

Yet another important principle of design, which reflects the determinate character of modular structure, consists of conservation or an increase in the symmetry of the "seed" cluster (the structure of the preceding "homologue") due to further jointing of modules using binary symmetry operations ($\bar{1}$, 2, *m*). The disturbance of periodicity in the cluster structure is attained by using those binary symmetry operations which are absent in the space group of the crystal and correspond to the local twinning of modules.

The modular design of clusters allows creation of an "idealized" structure, which is inevitably strained because of the use of (i) binary symmetry operations absent in the space group of the crystal and (ii) "internal" coordinates (bond lengths, bond angles, and torsion angles) characteristic of the crystalline state rather than twins. Admissible changes in these parameters and the removal of some vertices of the modules (see Fig. 2, *c*) without disrupting the connectivity of two-dimensional modular loops is the problem of the next step of modular design (passage from idealized structures to real structures of clusters).

The role of polyhedral representation of structures in modular design. The choice of the elements of design, namely, polyhedra of simplices and modules, which meet two conditions for cluster stability (the maximum density and total jointing of all bonds) and correspond to stereochemical invariants of the local order of crystal structures, predetermines the type of representation of the structures to be created. This is the polyhedral representation in which the atoms and chemical bonds are replaced by the vertices and edges of polyhedra, respectively. It should be noted that the formation of crystal chemistry is associated with the use of polyhedral representation of crystal structures. It was the polyhedral representation of structures that made it possible "to see the wood for the trees" and to formulate[37] five crystal-chemical rules of structural organization of crystals. The structural motifs isolated by Belov who used polyhedral representation of structures provided the basis for crystal-chemical classification[15] and allowed unambiguous isolation of "crystalline" modules in structures.[8] Using the polyhedral representation, one can unambiguously determine the site for the addition of atoms or an atomic group necessary for the completion of modules or simplices to the "seed' cluster and to determine binary symmetry operations and relevant parameters characterizing the algorithms of modular design of clusters.

Binary symmetry operations and relevant parameters of the algorithms of modular design of metal cluster structures. In the crystal structures which can be created using one type of modules, the edges of the modules are determined by "internal" coordinates, which reflect peculiarities of stereochemistry of the bonds in a given substance in the equilibrium state. In the case of polymodular combinatorial structures of amorphous substances assembled from the modules of possible polymorphous crystalline modifications of the substance,[28] it is clearly recognized that strong local disturbance of the bond stereochemistry is hardly probable since amorphous solids are rather stable. Binary symmetry operations, which disturb periodicity and correspond to local twinning of modules, also have little effect on the position of the energy minimum of the crystalline phase since phase transitions in crystals is often accompanied by twinning. It should be remembered that binary symmetry operations used for the jointing of modules can be the same as symmetry operations for the atoms in the modules. In the fcc and hcp structures, R-modules are jointed along the [0001] direction using different binary symmetry operations ($\bar{1}$, 2, *m*; see Fig. 4, *a* and *b*, respectively). To characterize the local order in the fcc and hexagonal close packings, it is sufficient to know the symmetry of jointing of two simplices of one type with one simplex of another type (hatched) or, which is the same, only a part of the Delone star corresponding to the first coordination spheres of the fcc and hexagonal close packings (see Fig. 1, *b*, *c*). In the fcc structure (see Fig. 4, *c*), passage from the edge-to-edge (along the ⟨110⟩ direction) to the face-by-face type of jointing of the octahedra in the columns parallel to the C_3 axis (see Fig. 4, *d*, *e*) means a local disturbance of periodicity of the fcc packing in this direction. For the polyhedra in columns joined at vertices, difference in binary symme-

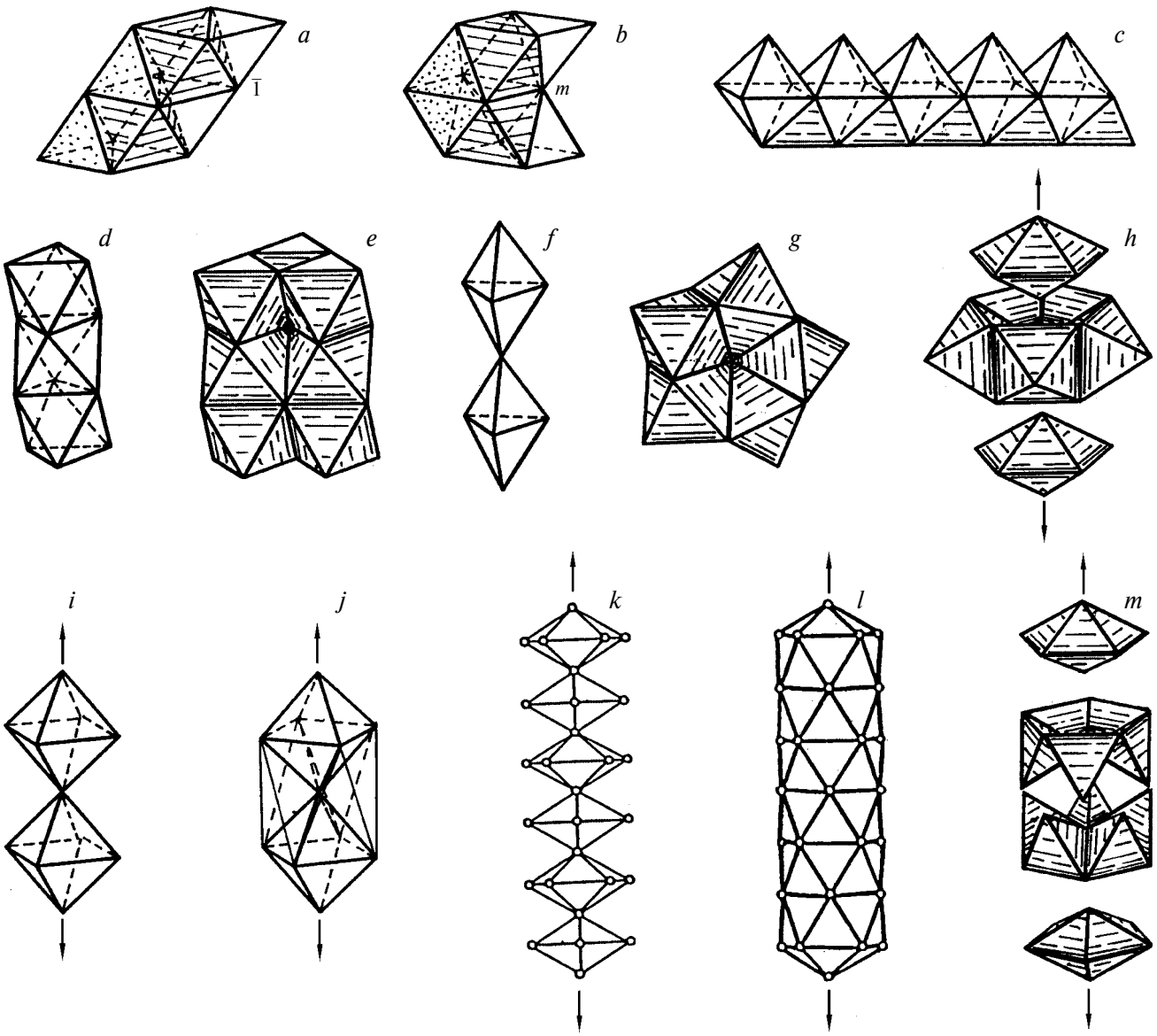

Fig. 4. Symmetric combinations of simplices and D_{5h}-modules which characterize: the local order in the fcc (*a*, *c*) and hcp (*b*, *d*—*f*) crystal structures; binary symmetry operation *m* in the radial (along C_5 axes) chain of D_{5h}-modules of icosahedral clusters (*g*, *h*); binary symmetry operations *m* and $\bar{1}$ in the chain of octahedra (*i*, *j*); binary symmetry operation $\bar{1}$ in the chain of D_{5h}-modules with algorithm $(\bar{1})_p$ in the structure of a rod from interpenetrating icosahedra (*k*, *l*); and binary symmetry operation $\bar{1}$ in the fragment of a chain of D_{5h}-modules and tiling into tetrahedral simplices corresponding to this operation (*m*).

try operations can be described using the parameter θ. In the hexagonal close crystal packing, the tetrahedra (see Fig. 4, *f*) join to form columns pairwise both by faces and at vertices (binary symmetry operation *m*, θ = 0°). The same θ value for a pair of octahedra joined at a vertex by binary symmetry operations $\bar{1}$ and *m* (see Fig. 4, *i*) is typical of BaO_2 crystals assuming that the shared vertex is occupied by Ba, while the remaining vertices are occupied by O atoms.[15] A polyhedron (see Fig. 4, *j*) formed at θ = 45° (binary symmetry operation C_2) is characteristic of non-Euclidean structures and corresponds to one of Bernal's "canonical holes" (see Fig. 3, *f*).[20]

In the fcc structure (see Fig. 4, *c*), chains of five octahedra joined to one another by edges and those of five tetrahedra joined at vertices along the [110] direction can be rolled into closed pentagonal cycles using binary symmetry operation *m* (see Fig. 4, *g*, *h*). Pentacycles of octahedra fill the interstice between the pentacycles of tetrahedra (D_{5h}-modules), thus forming rods with *p* 5/*m m* symmetry (see Fig. 4, *h*) in which D_{5h}-modules are joined at vertices using binary symmetry operation *m* (θ = 0°). Despite the fact that the pentagonal symmetry is forbidden in the lattice crystallography, these rods are compatible with the fcc crystal structures in icosahedral complex twins (see Section

"Clusters with $\bar{1}(m)_p$ radial algorithms as complex twins of the fcc crystals with color icosahedral symmetry"). The binary symmetry operation $\bar{1}$ used for joining the D_{5h}-modules at vertices to form a rod with $p\bar{1}0m2$ symmetry ($\theta = 36°$) corresponds to the formation of a column of interpenetrating icosahedra (see Fig. 4, *k*, *l*). The non-Euclidean nature of this structure is confirmed by the fact that the interstice between two D_{5h}-modules along the C_5 axis is filled with ten tetrahedral simplices (see Fig. 4, *m*), so that each icosahedron is a Delone star of twenty tetrahedral simplices. Rod-like structures comprising three interpenetrating icosahedra were found in $(MePhP)_{10}Au_{12}Ag_{13}Br_9$ clusters.[38] Algorithms of these structures use the parameter θ with the values 0°(*m*), 36°($\bar{1}$), and 9°(C_2),[39,40] which is analogous to the parameter θ.

Radial algorithms of modular design of metal clusters. The "seed," or center, of any cluster with a global icosahedral symmetry is always the 13-atom icosahedron. Twelve equivalent C_5 axes formed by chains of D_{5h}-modules joined at vertices using binary symmetry operations $\bar{1}$ or *m* pass through the vertices of this icosahedron. One-dimensional sequences of these operations with parameters $\theta = 36°$ for $\bar{1}$ and $\theta = 0°$ for *m* are the algorithms of modular design of icosahedral clusters. The notation of a radial algorithm begins with $\bar{1}$ at the common center of any icosahedral cluster and the sequences of binary symmetry operations (different for different icosahedral clusters) are given in parentheses. For instance, the design algorithm of the 561-atom cluster corresponding to the Chini series of magic numbers can be written as $\bar{1}_{D_{5h}}$ ($m_{D_{5h}}$ $m_{D_{5h}}$ $m_{D_{5h}}$ $m_{D_{5h}}$) or, briefly, $\bar{1}(m)_4$.

Let us show that such a notation of the one-dimensional algorithm of modular design does describe the structure of icosahedral clusters. The angles between the adjacent C_5 axes in the icosahedron are equal to 63.5°, which nearly coincides with the angle of 60° between the directions of adjacent C_2 axes (⟨110⟩) in the fcc structure. The number of C_2 axes in the latter structure is equal to that of C_5 axes in the icosahedron (12). It is this similarity between the C_2 axes in the fcc structure and the C_5 axes in the icosahedron that is responsible for the possibility of icosahedral complex twins with (111)/(111) twin boundaries to be formed in the fcc structure and in diamond.[41] The difference in the angles between the corresponding axes is the cause of strain in these twins, despite the completely coherent structure of the (111)/(111) boundaries. However, unlike other types of icosahedral clusters (see Section "Icosahedral metal clusters with one-dimensional radial algorithms"), the strain in icosahedral twins with common algorithm $\bar{1}(m)_p$ will also decrease with increase in their size because the angular discrepancies do not increase with growing. Icosahedral twins are formed by twenty tetrahedral sectors of the fcc structure. In these sectors, each edge consist of a chain of the edges of tetrahedral simplices (Fig. 5, *a*). In icosahedral clusters, chains of tetrahedral simplices on the edges of five fcc sectors parallel to the same C_5 axis (see Fig. 5, *a*) form chains of quinary twins (D_{5h}-modules, see Fig. 5, *c*) along all 12 C_5 axes, which alternate with pentacycles (also cyclic quinary twins) of octahedra (see Fig. 4, *g*), thus forming rods with $p\,5/m\,m$ symmetry using binary symmetry operations *m* with $\theta = 0°$ (see Fig. 4, *e*). The use of binary symmetry operations $\bar{1}$ ($\theta = 36°$) for linking of D_{5h}-modules along C_5 axes (see Fig. 5, *b*) leads to filling of the interstices between the modules by ten tetrahedral simplices (see Fig. 4, *m*) and to the formation of the layers of non-Euclidean structures comprised of distorted icosahedra (see Section "Icosahedral clusters with regular mixed radial algorithm $\bar{1}(m\bar{1})_p$"), which imposes restrictions on further growth of icosahedral clusters with algorithms $\bar{1}(\bar{1})_p$, $\bar{1}(m\bar{1})_p$, *etc.*

Tetrahedral fragments of the fcc structures (see Fig. 5, *a*) can be coherently embedded in the sectors whose edges are rods of D_{5h}-modules with $p\,5/m\,m$ symmetry and $\bar{1}(m)_p$ algorithms parallel to the C_5 axes (see Fig. 5, *c*—*e*). The size of icosahedral clusters can be determined using the parameter $r = p + 1$ of radial algorithms $\bar{1}(m)_p$, $1(\bar{1})_p$, $\bar{1}(m\bar{1})$, where *p* is the number of the symbols of binary symmetry operations given in parentheses. The number, *r*, of D_{5h}-modules along the radial direction with respect to the C_5 axis, including the D_{5h}-module in the central icosahedron (see Fig. 5, *b*—*f*), equals $p + 1$. The height of the D_{5h}-module along its C_5 axis (see Fig. 3, *b*, *c* and Fig. 4, *h*) is equal to the edge length of the tetrahedral simplex, *i.e.*, the mean bond length (~2.6 Å for transition metals). Therefore, the diameter of the sphere circumscribed about icosahedral cluster with any algorithm is $2(p + 1) \cdot 2.6$ Å = $5.2(p + 1)$ Å.

It should be remembered that all tetrahedral sectors of the fcc structures have edges of the same length, which is expressed through either the number of edges of tetrahedral simplices or the number of D_{5h}-modules. The parameter $r = (p + 1)$ equal to the number of D_{5h}-modules is also equal to the number of layers of the fcc close packing in the tetrahedral sectors of icosahedral clusters with the $\bar{1}(m)_p$ radial algorithm. Therefore, the parameter *r* of the radial algorithm corresponds to the parameter $K - 1$ in the formula[35] for calculating the number of atoms in the icosahedral clusters of the Chini series with the algorithm $\bar{1}(m)_p$

$$N = (10/3)K^3 - 5K^2 + (11/3)K - 1. \qquad (1)$$

The parameter *r* of the $\bar{1}(m)_p$ radial algorithm corresponds to the parameter *n* in the formula used for determination of the number of atoms in icosahedral clusters of the same Chini series.[34]

$$N = (1/3)(2n + 1)(5n^2 + 5n + 3). \qquad (2)$$

The equality of the parameters *r* and *n* is explained by the fact that they are equal to both the total number of D_{5h}-modules in the icosahedral clusters with the $\bar{1}$

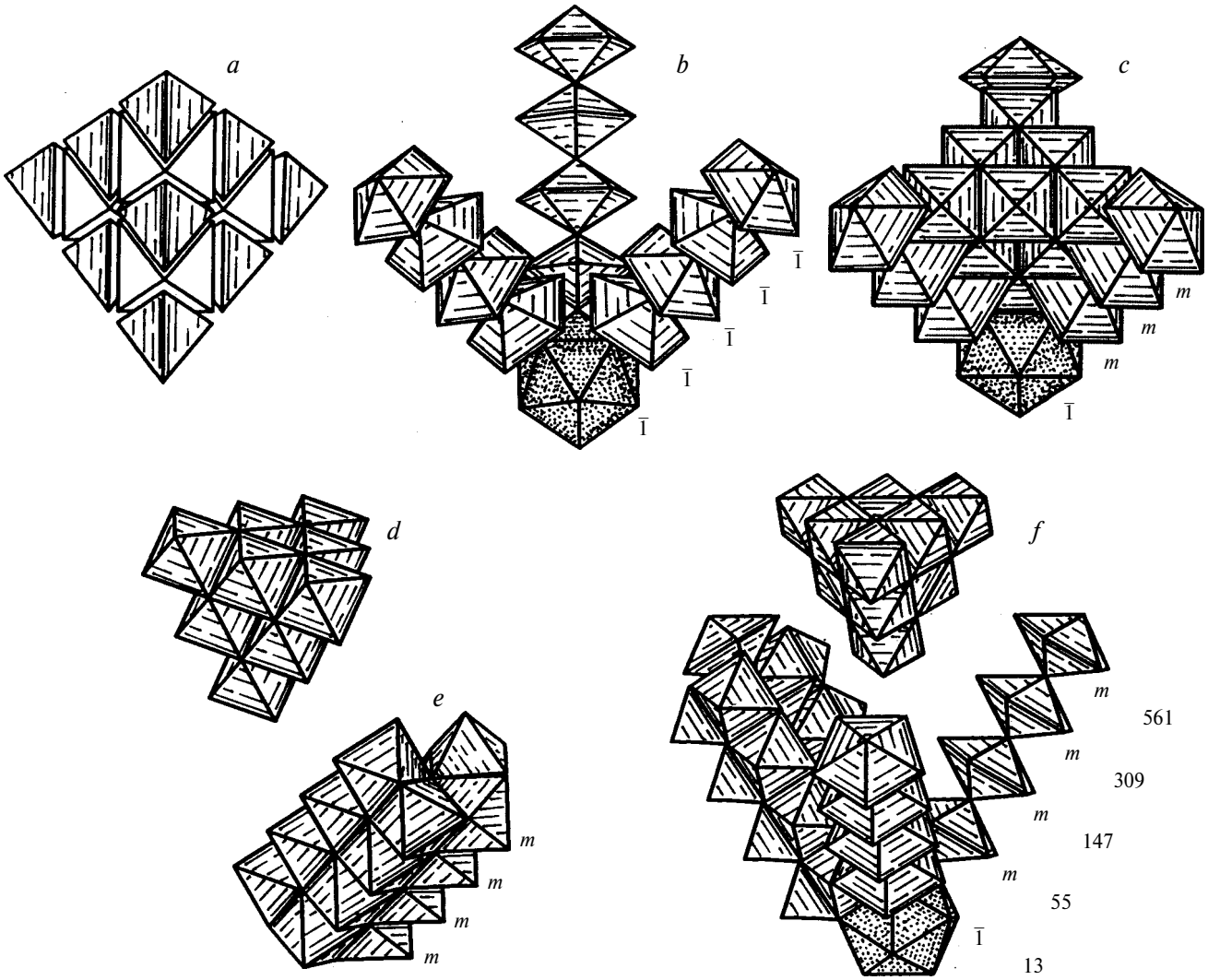

Fig. 5. One-dimensional algorithms: in the fragment of the fcc structure with tetrahedral morphology (*a*); in the chains of D_{5h}-modules in the icosahedral cluster with the $\bar{1}(\bar{1})_4$ algorithm along three axes of the central icosahedron shown by dots (*b*) and in the fragment of the fcc structure with three joined chains of D_{5h}-modules with $\bar{1}(m)_1$ algorithm (*c*); in the column of pentacycles of octahedral simplices (for clarity, one octahedron in each simplex is removed) and in jointed fragments of the fcc structures in which the octahedra located on the edges of the fragment form these pentacycles (*d*); in the chains of algorithms along C_5 axes (*e*); and octahedral simplices of the fragments of the fcc structure, which fill the interstices between D_{5h}-modules in the chains along three C_5 axes in the octahedral simplices (*f*).

$(m)_p$ radial algorithm and the number of bonds on the edges that connect two adjacent C_5 axes in the icosahedral cluster. The parameter $K = n + 1$,[35] where $n = r$, corresponds to the number of atoms on the radii parallel to the C_5 axes and on the edges of the icosahedra with the $\bar{1}(m)_p$ algorithm.

Icosahedral metal clusters with one-dimensional radial algorithms

It is impossible to determine the structure of clusters from experimental data obtained by mass spectroscopy[10,35] as well as using information on ionization potentials[6,10] and melting temperatures[11] even if the clusters correspond to the same series of magic numbers (*e.g.*, the Chini series), since often their morphology cannot be reliably established by modern microscopy techniques. The point is that the volumes of several regular polyhedra with equilateral triangular and square faces (cubic and hexagonal cuboctahedra, Fig. 6, *g*, *j* and a combination of a pentagonal prism and bipyramid, see Fig. 6, *i*) are nearly equal to the volume of an icosahedron with edges of the same length (see Fig. 6, *h*). Therefore, the Chini magic numbers may correspond not only to icosahedral clusters but also nanoparticles with the morphology of these polyhedra. The number of atoms in them is determined using formula (1), where K is the number of atoms on the edges of these polyhedra.[35]

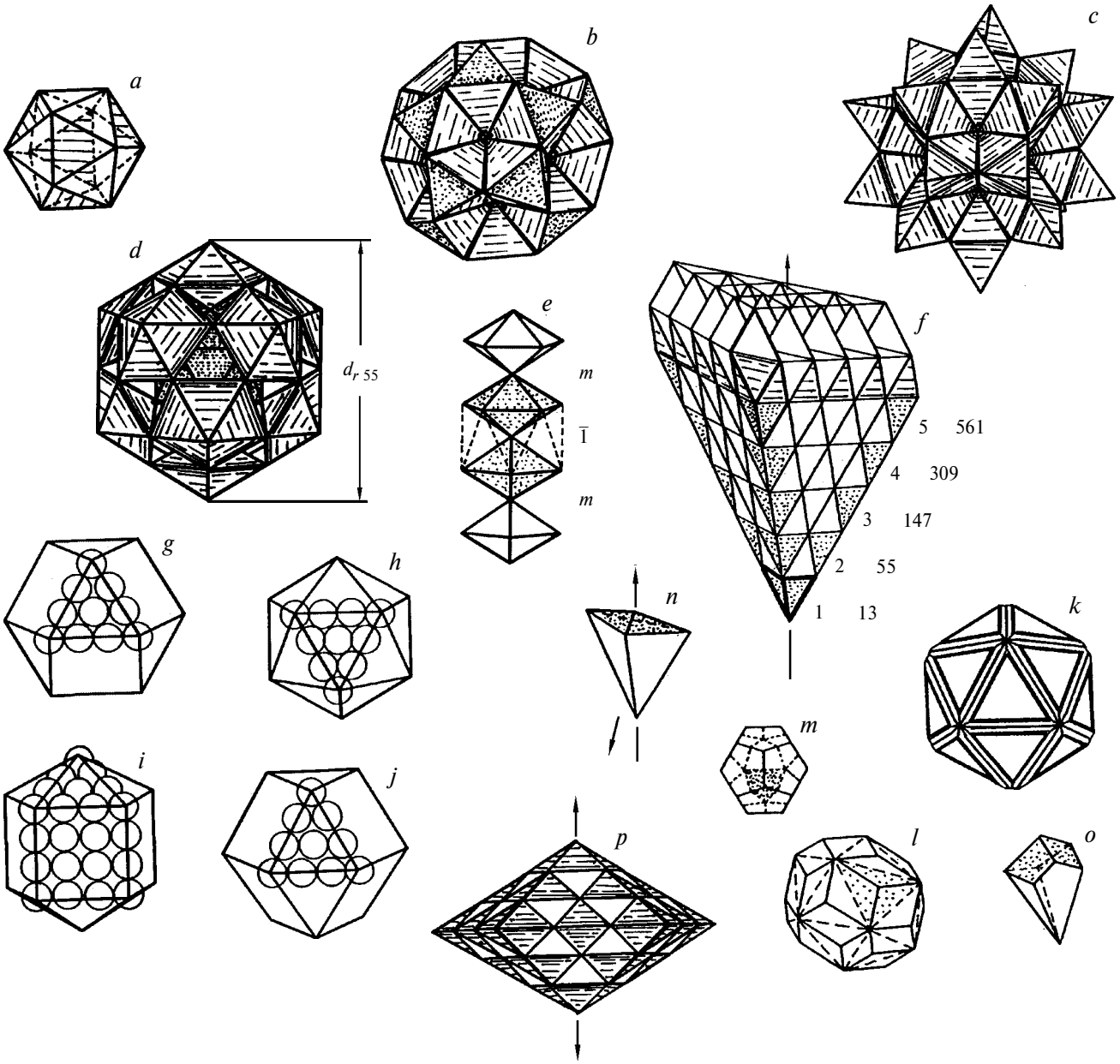

Fig. 6. Structure of icosahedral metal clusters of the Chini series with radial algorithm $\bar{1}(m)_p$: the central icosahedron with four tetrahedral simplices (hatched) of the same orientation in the cubic setting (*a*); the 43-atom cluster (*b*); the Delone star from R-modules (*R*-cells of the fcc structure) corresponding to the 63-atom cluster (*c*); the Mackay icosahedron (*d*) and the chain of D_{5h}-modules along all 12 C_5 axes, corresponding to its radial algorithm $\bar{1}(m)_1$ (*e*); tetrahedral fragments of the fcc structure, which form all icosahedral modules with algorithms $\bar{1}(m)_p$ (*f*); regular polyhedra ($K = 4$) containing the equal number of atoms at the same parameters (*g*—*j*); morphological forms derived from the ideal icosahedral morphology of the Chini clusters generated in the development of nonplanar growth surface of tetrahedral fcc clusters sectors (*k*—*m*); trigonal pyramids of the growth surfaces of tetrahedral sectors (*n*, *o*) responsible for triacontahedral (*l*) and pentagondodecahedral (*m*) habits of icosahedral clusters; and quinary twin (*p*) self-similar to D_{5h}-module, which is a uniaxial analog of icosahedral clusters with the $\bar{1}(m)_p$ algorithm ($p = 3$).

Icosahedral clusters with the $\bar{1}(m)_p$ radial algorithm corresponding to the "homologous series" with the Chini magic numbers can have different types of morphology. If so, the number of atoms in the clusters whose morphology differs from ideal icosahedral can be different from the Chini magic numbers. Therefore, it is important to establish the type of algorithm of icosahedral clusters rather than their correspondence to a particular series of magic numbers. The type of radial algorithm and relevant binary symmetry operations are responsible for the Euclidean or non-Euclidean nature of the layers of icosahedral clusters and, hence, for the possibility of the development of a specified family of clusters and their limiting size. The types of radial algorithms define

the system of parametric classification of icosahedral clusters and manifest themselves in the peculiarities of their internal structure. Apart from the polyhedral representation of clusters used in modular design, when only the bonds on the surface of the clusters can be seen as modular polyhedra, one can use other projections in order to see all bonds in the cluster structure. This opens new possibilities for studying the regularities of the internal structure of clusters, which can make themselves evident in the peculiarities of the radial distribution curves obtained by diffraction methods.

Clusters with $\bar{1}(m)_p$ radial algorithms as complex twins of fcc crystals with color icosahedral symmetry. Genesis of all icosahedral clusters begins with the 13-atom icosahedron, which is the Delone star formed only by tetrahedral simplices (see Fig. 6, *a*). All clusters with the $\bar{1}(m)_p$ radial algorithm, corresponding to the "homologous series" with the Chini magic numbers, are formed due to joining of 20 octahedral simplices to all faces of the central icosahedron (see Fig. 6, *b*). The number of atoms in such a cluster is 43, since each octahedron does not share three atoms with the central icosahedron but simultaneously shares them with two octahedra [$13 + (3 \cdot 20)/2 = 43$]. In the 43-atom cluster, 20 octahedra form 12 pentagonal cycles (Fig. 4, *g*) so that twelve D_{5h}-modules can be embedded in their "craters"; in this case, each module adds only one unshared vertex (see Fig. 4, *h*). This results in the famous 55-atom cluster, or the Mackay icosahedron[42] (see Fig. 6, *d*). In this cluster, chains of D_{5h}-modules joined at vertices (see Fig. 6, *e*) using binary symmetry operations according to the ${}_{D_{5h}}m_{D_{5h}}\bar{1}_{D_{5h}}m_{D_{5h}}$ algorithm can be isolated along any of the six diameters parallel to C_5 axes. Ignoring relaxation of the bond lengths, the diameter of the Mackay icosahedron ($d_{r\ 55}$) is nearly equal to the height of four D_{5h}-modules or four interatomic distances (R(M—M) ≈ 2.6 Å): $d_{r\ 55} = 4 \cdot 2.6$ Å ≈ 10 Å. Joining of 20 tetrahedral simplices shown by dots in Fig. 6, *b* to all faces of the octahedra in the 43-atom cluster results in a 63-atom cluster (see Fig. 6, *c*), which is a Delone star of 20 R-modules (see Fig. 1, *d*) with the common vertex at the center of the cluster. Each R-module equivalent to the rhombohedral unit cell in the fcc structure is formed by one octahedron and two tetrahedra, one of which is a part of the central icosahedron. Further development of icosahedral clusters with the $\bar{1}(m)_p$ radial algorithm can be represented as a synchronous, layer-by-layer growth of all 20 tetrahedral sectors with fcc structure. This results in a complex twin with coherent (111)/(111) boundaries along all edges of the icosahedron. One of the 20 sectors of the fcc crystal, where tetrahedral simplices are shown by dots on three edges, is shown in Fig. 6, *f*. A chain of D_{5h}-modules joined at vertices using binary symmetry operations m ($\theta = 0°$) is formed along the C_5 axis in the cyclic twin comprised of five fcc sectors (see Fig. 5, *c*, *f*). The lowest tetrahedron at the vertex of the fcc sector (shown by solid lines in Fig. 6, *f*) is a part of the central icosahedron of the cluster. The numbers on the sector edge near each vertex of tetrahedral simplices are equal to (i) the number of bonds or edges of tetrahedral simplices along the edges of the icosahedral cluster and the C_5 axes and (ii) the total number of D_{5h}-modules (r) in the $\bar{1}(m)_p$ algorithm; they are also the parameters $r = n = p + 1$ and enumerate the Chini magic numbers as follows: 1 (13); 2 (55); 3 (147); 4 (309); 5 (561)... The parameters p and n which appeared in the $\bar{1}(m)_p$ radial algorithm and in formula (2) determine the total number of atoms in these icosahedral clusters. The diameters (along C_5 axes) of icosahedral clusters with the $\bar{1}(m)_p$ algorithm are calculated using the formula $d_r = 2rR$(M—M), where R(M—M) = 2.6 Å and $r = p + 1 = n$.

It is not to be supposed that all 20 tetrahedral sectors in the complex icosahedral twin have different orientations. Since the T-23 point symmetry group is the subgroup of the icosahedral point group symmetry, the complex twin with the $\bar{1}(m)_p$ algorithm is in fact a quinary intergrowth twin. In such an object consisting of five interpenetrating crystals, 20 tetrahedral sectors are divided into five groups of four crystal sectors with the same orientation. One group is shown by dashed lines in Fig. 6, *a*. The full symmetry of the icosahedral clusters with the $\bar{1}(m)_p$ algorithm and corresponding to the Chini magic numbers is described by color symmetry of index 5 in the form $m\bar{3}\bar{5}^{(5)}$, where $5^{(5)}$ is the axis of color symmetry.[43—45]

As was mentioned above, icosahedral clusters with the $\bar{1}(m)_p$ radial algorithm can have different types of morphology. However, the number of atoms in such clusters will correspond to the Chini magic numbers. As can be seen in Fig. 6, *f*, the seventh layer of the tetrahedral sector is not completed, which results in the appearance of small ditches on all edges and small "craters" at the vertices of icosahedral clusters (see Fig. 6, *k*). Apart from such a "faulty" change in ideal icosahedral shape of the clusters with the $\bar{1}(m)_p$ algorithm, a complete change of the icosahedral morphology and its transformation into triacontahedral and pentagondodecahedral forms is possible (traces of twin boundaries are shown by dotted lines in Fig. 6, *l*, *m*). The appearance of these forms of clusters requires the corresponding pyramidal terrace-like faces to be grown on the growth surface of tetrahedral sectors (see Fig. 6, *n*, *o*) as a prerequisite; however, their edges will have different orientations with respect to the edges of tetrahedral sectors of the cluster.

If the $\bar{1}(m)_p$ algorithm is realized along only one out of twelve C_5 axes, two forms of quinary intergrowth twins with $5^{(5)}/m\ m'$ symmetry (m' denotes the two-color symmetry plane) can be created. The first form is a combination of the pentagonal prism formed by the {100} faces and a bipyramid the {111} faces (see Fig. 6, *i*). The second form is self-similar to the D_{5h}-module at a $1 : r$ ratio (see Fig. 6, *p*). All types of clusters with the $\bar{1}(m)_p$ algorithm considered in this review are the Euclidean structures; therefore, they can grow to reach macroscopic size.

Non-Euclidean structures of icosahedral clusters with radial algorithm $\bar{1}(\bar{1})_p$. In contrast to the clusters with the $\bar{1}(m)_p$ algorithm, twenty tetrahedra having one unshared vertex each rather than octahedra are added to all faces of the central 13-atom icosahedron (Fig. 7, *a*) in the clusters with the $\bar{1}(\bar{1})_p$ algorithm. This results in a 33-atom cluster. The vertices of the twenty joined tetrahedra correspond to those of a pentagondodecahedron whose edges are shown by dotted lines in Fig. 7, *b*. In the 33-atom cluster one can join twelve D_{5h}-modules (see Fig. 7, *c*, *d*) on the C_5 axes perpendicular to the faces of the pentagondodecahedron. Only one out of seven atoms in each of the twelve D_{5h}-modules is unshared with the vertices of tetrahedra. Eventually, the 45-atom cluster ($33 + 12 \cdot 1 = 45$) is formed. It is characterized by the triacontahedral morphology (see Fig. 7, *e*, *g*) and $\bar{1}(\bar{1})_1$ algorithm. The diameter (along C_5 axes) of this cluster is $2 \cdot 2p \cdot R(\text{M—M}) = 4R(\text{M—M})$, which coincides with the diameter of the Mackay icosahedron with the $\bar{1}(m)_1$ algorithm (see Fig. 7, *i*). Only the tetrahedral simplicial tiling (see Fig. 4, *m* and Fig. 7, *d*) characteristic of non-Euclidean structures corresponds to binary symmetry operation $\bar{1}$ of joining of two D_{5h}-modules in the radial algorithm. What is the reason for the difference in the number of atoms between the non-Euclidean 45-atom cluster and Euclidean 55-atom cluster with nearly equal volumes?

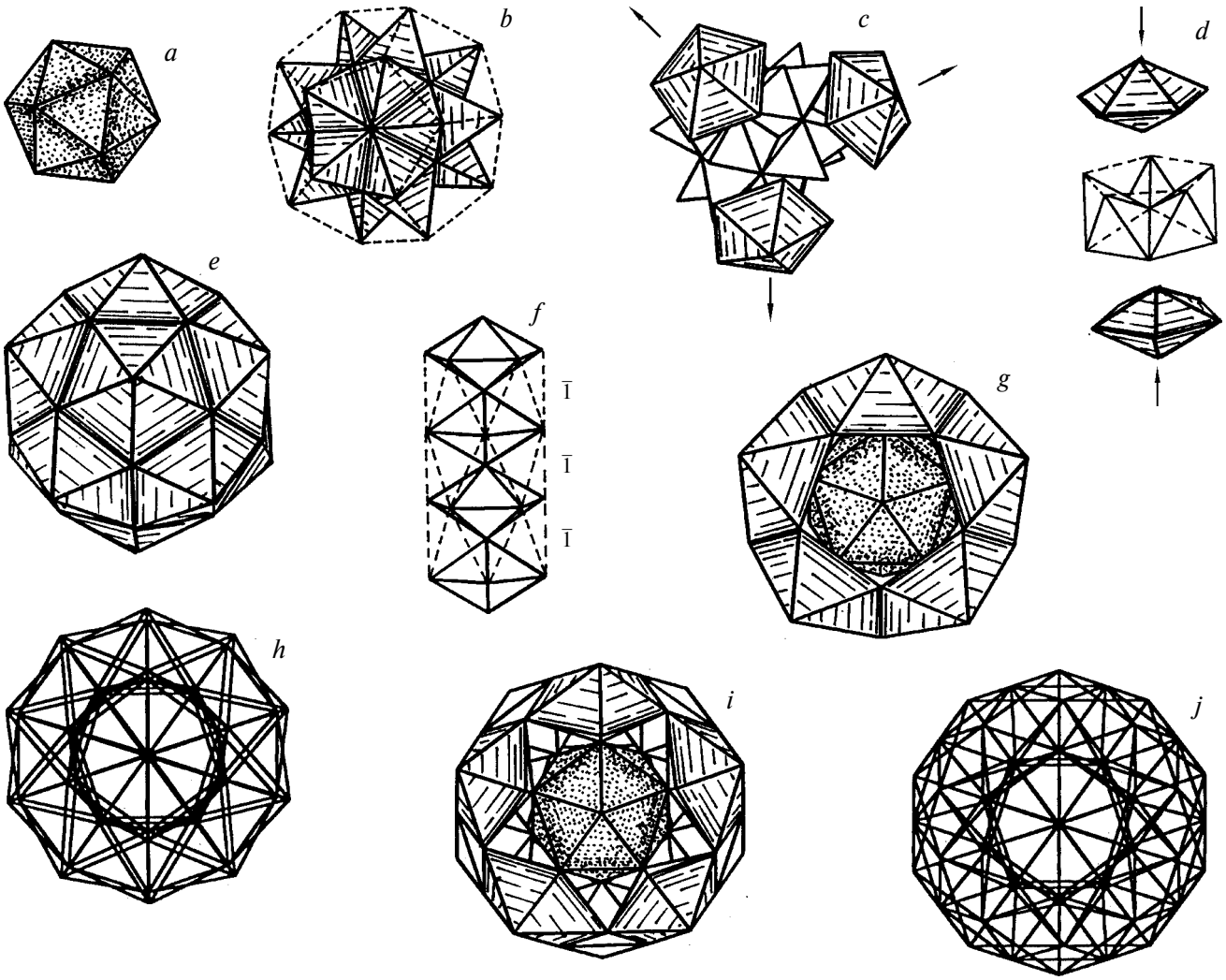

Fig. 7. Non-Euclidean icosahedral clusters with the $\bar{1}(\bar{1})_p$, $p \leq 2$ radial algorithm: the central icosahedron (*a*); the 33-atom cluster (*b*) with pentagondodecahedral morphology (faces are shown by dotted lines); positions on C_5 axes to which additional 12 D_{5h}-modules can be joined to the 33-atom cluster (*c*); the non-Euclidean tetrahedral simplicial tiling corresponding to the binary symmetry operation $\bar{1}$ in the radial algorithm (*d*); the 45-atom cluster and the chain of D_{5h}-modules (*e*) along its C_5 axes corresponding to the $\bar{1}(\bar{1})_1$ algorithm; a chain of D_{5h}-modules (*f*) along the cluster diameter parallel to the C_5 axis corresponding to the $\bar{1}(\bar{1})_1$ radial algorithm; positions of twelve outermost D_{5h}-modules in the structures of the 45-atom cluster (*g*) and the 55-atom Mackay icosahedron (*i*); and projections of all bonds along C_5 axes in the structures of these clusters (*h*, *j*).

The full algorithm of the 45-atom cluster, $\bar{1}(\bar{1})_1$, corresponding to three interpenetrating icosahedra along the C_5 axes, includes operations on four D_{5h}-modules joined at vertices by binary symmetry operation $\bar{1}$ ($\theta = 36°$) and shown in Fig. 7, *f*. When comparing the projections of all bonds in the 45-atom cluster (see Fig. 7, *h*) and the Euclidean 55-atom Mackay icosahedron (see Fig. 7, *j*) on the C_5 axes, the non-Euclidean nature of the former makes itself evident in an appreciable (by ~10%) lengthening of non-radial bonds and fuzziness of multiple bond intersections corresponding to the atomic positions in the structure due to large structural distortions. It is known that fragments of non-Euclidean structures cannot be embedded without distortions in the three-dimensional Euclidean space;[46] therefore, such packings are deliberately called packings of "soft spheres,"[13] since their diameters can increase or decrease in order to relax an inevitable strain. The ratio of the numbers of atoms in the icosahedral clusters with the $\bar{1}(m)$ and $\bar{1}(\bar{1})$ algorithms is 55/45 = 1.22. The lengthening of non-radial bonds within the limits of 10% compared to the normal bond length compensates the difference in the number of atoms (55 *vs.* 45) in these icosahedral clusters with nearly equal volumes.

The 45-atom cluster is the only representative of the series of clusters with the $\bar{1}(\bar{1})_p$ algorithm ($p = 1$) and constitutes the central part of the structure of the four-dimensional icosahedron (the {3,3,5} polytope) with finite number of atoms.[47] The structure of the {3,3,5} polytope comprised of interpenetrating icosahedra is such that (1) each bond is the C_5 axis in the D_{5h}-module, (2) each atom is the center of the 13-atom icosahedron, and (3) the 30/11 helices are the Bernal chains of tetrahedra.[20]

Icosahedral clusters with regular mixed radial algorithm $\bar{1}(m\bar{1})_p$. In addition to the radial algorithms which include binary symmetry operations m and $\bar{1}$ used for joining of D_{5h}-modules along C_5 axes outside the central icosahedron, ($\bar{1}(m)_p$) and ($\bar{1}(\bar{1})_1$), there are two other types of mixed radial algorithms, namely, regular algorithms $\bar{1}(m\bar{1})_p$ and an irregular algorithm $\bar{1}(m\,m\bar{1}m)$. The presence of more than one binary symmetry operation $\bar{1}$ in the algorithm is an indicator of the non-Euclidean tetrahedral tilings of at least one layer of the cluster in addition to the central icosahedron. It should be remembered that binary symmetry operations m in the algorithm correspond to the layers with the Euclidean crystal structure built of octahedral and tetrahedral simplices. With increase in the separation between the non-Euclidean layers and the cluster center, the distortions of the bond lengths and strain will increase according to the position of binary symmetry operation $\bar{1}$ in the radial algorithm. Unlike the $\bar{1}(m\bar{1})_p$ algorithm realized in the 127- and 381-atom clusters, the $\bar{1}(\bar{1}m)_p$ algorithm cannot be realized for reasons of a fundamental nature. In the case of the 45-atom cluster with the $\bar{1}(\bar{1})_1$ algorithm (see Fig. 7, *e*), octahedra cannot be joined to the faces of 60 tetrahedral simplices on the cluster surface according to the $\bar{1}(\bar{1}m)$ algorithm without overlapping of the vertices of the octahedra since the angles between the faces in the triacontahedron (144°) are larger than in the icosahedron (138.2°).

The doubled radial algorithm $({}_{D_{5h}}\bar{1}_{D_{5h}}m)_{D_{5h}}\bar{1}_{D_{5h}}(m_{D_{5h}}\bar{1}_{D_{5h}})$ of the 127-atom cluster[13] corresponds to (i) a chain of D_{5h}-modules along the diameter parallel to the C_5 axis (Fig. 8, *a*) and (ii) a chain of icosahedra, which replace each pair of D_{5h}-modules joined by the binary symmetry operation $\bar{1}$ (see Fig. 8, *b*) in the algorithm. The "seed" of the 127-atom cluster is the 55-atom Mackay icosahedron with the $\bar{1}(m)_1$ radial algorithm which can be isolated in the doubled algorithm ${}_{D_{5h}}\bar{1}|_{D_{5h}}m_{D_{5h}}\bar{1}_{D_{5h}}m_{D_{5h}}|\bar{1}_{D_{5h}}$ corresponding to the diameter of the larger cluster. It is obvious that the D_{5h}-modules with six unshared vertices have to be joined to the Mackay icosahedron (see Fig. 6, *d* and Fig. 7, *i*) on all twelve C_5 axes to complete the structure of the 127-atom cluster: $55 + 12 \cdot (7 - 1) = 127$ (see Fig. 8, *a*—*c*).

The $(m\bar{1})$ cycle can be repeated in the $\bar{1}(m\bar{1})_2$ algorithm due to joining of 12 icosahedra along all the C_5 axes by binary symmetry operation m. Analysis of the full algorithm corresponding to the diameter of the cluster along the C_5 axis, $({}_{D_{5h}}\bar{1}_{D_{5h}})m_{D_{5h}}\bar{1}_{D_{5h}}m({}_{D_{5h}}\bar{1}_{D_{5h}})m_{D_{5h}}\bar{1}_{D_{5h}}m({}_{D_{5h}}\bar{1}_{D_{5h}})$, allows isolation of the algorithms corresponding to three icosahedra, namely, two icosahedra at both ends of the diameter and one icosahedron at the center of the cluster. These algorithms are given in parentheses. The "block diagram" of the full algorithm is shown in Fig. 8, *b* in which the icosahedra joined to the 127-atom cluster by binary symmetry operation m ($\theta = 0°$) are shown by dots. The total number of atoms in the icosahedral cluster with the $\bar{1}(m\bar{1})_2$ radial algorithm is 381, which corresponds to the structure of an icosahedral cluster reported in Ref. 13. The number of atoms in this cluster is calculated as follows. The 13-atom icosahedra with 12 unshared vertices are joined to the 127-atom icosahedron on all twelve C_5 axes: $12 \cdot (13 - 1) = 144$. The formation of the non-Euclidean layer corresponding to binary symmetry operation $\bar{1}$ causes joining of twenty distorted 13-atom icosahedra instead of octahedra and tetrahedra along all C_3 axes in the tetrahedral sectors of the icosahedral cluster with the $\bar{1}(m\bar{1})_2$ algorithm (see Fig. 8, *d*, *e*). These 13-atom icosahedra have three unshared vertices each (shown by heavy dots in Fig. 8, *d*). Three vertices on the lower face of each icosahedron joined on the C_3 axes are shared with the icosahedra of the 127-atom cluster located on the C_5 axes (shown by circles in Fig. 8, *c*). In addition, each icosahedron joined on the C_3 axes shares three vertices with two icosahedra shown by circles in Fig. 8, *c*, *e*. The icosahedra located on the C_5 axes are shown by dashed lines (Fig. 8, *c*—*e*). Thus, the joining of 12 icosahedra on the C_5 axes and 20 icosahedra on the C_3 axes to the 127-atom cluster results in a 381-atom cluster ($127 + 12 \cdot (13 - 1) + 20 \cdot (3 + 3/2) + 20 \cdot 1 = 381$). In this sum, twenty atoms

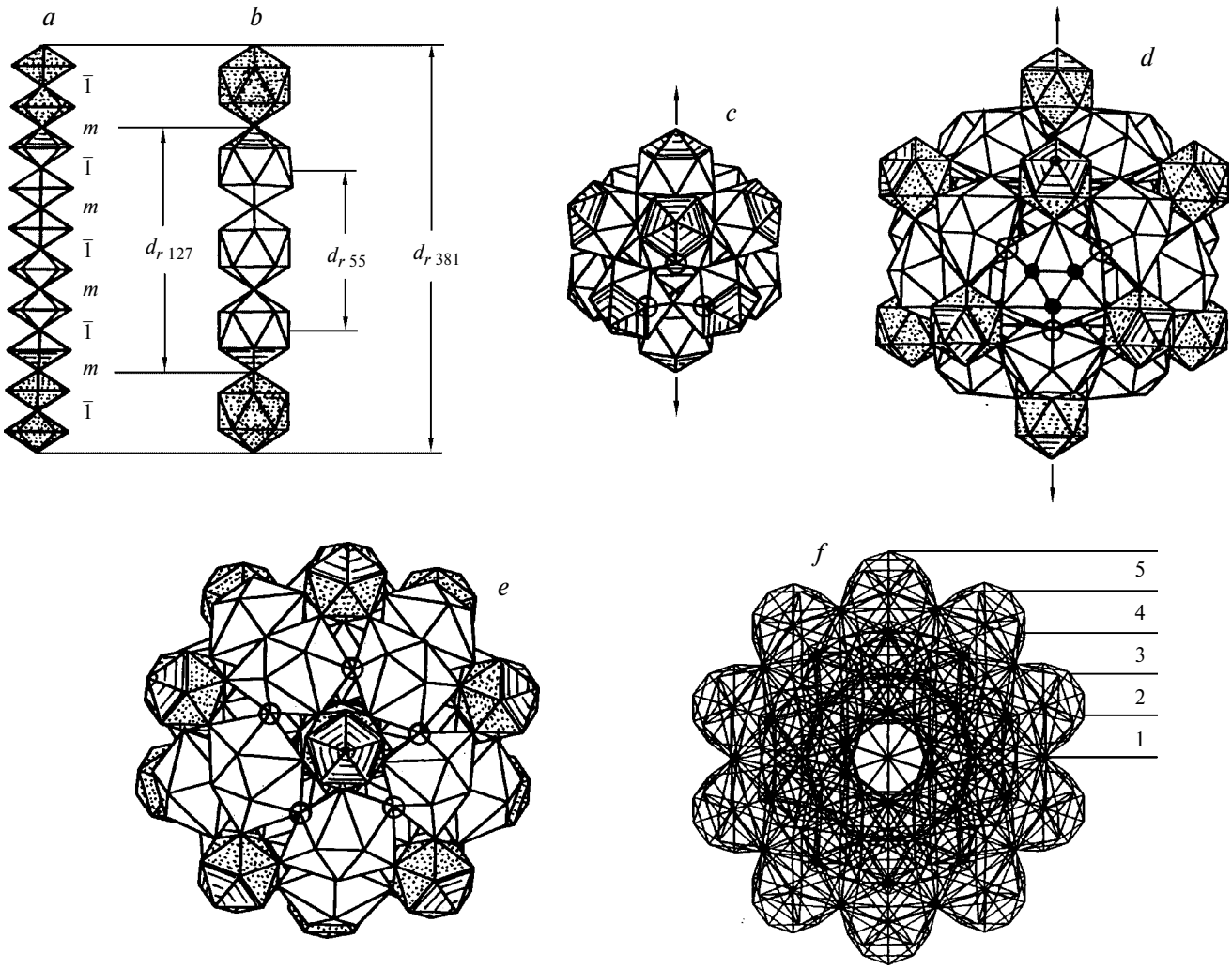

Fig. 8. Icosahedral clusters with the $\bar{1}(m\bar{1})_p$ radial algorithm ($p \leq 2$): chains of D_{5h}-modules (*a*) and chains of icosahedra (*b*) from D_{5h}-modules corresponding to the full $\bar{1}(m\bar{1}m\bar{1}m\bar{1}m\bar{1})$ algorithm; the 127-atom cluster (*c*), the C_5 axis parallel to the drawing plane and one of the twelve chains of icosahedra (*b*) is shown by arrows; the 381-atom cluster in different settings: with C_5 axis parallel to the drawing plane (*d*) and along the C_5 axis (*e*); and the projection of all bonds in the structure of the 381-atom cluster along the C_5 axis (*f*).

$(20 \cdot 1)$ correspond to the atoms at the centers of twenty icosahedra on C_3 axes. The diameter of the 381-atom cluster along the C_5 axis is equal to the length of the chain of ten D_{5h}-modules (26 Å). The projection of the 381-atom cluster along the C_5 axis shows all bonds and atomic positions (the latter as multiple bond intersections) in the structure (see Fig. 8, *f*). Here, four equidistant rings formed by "equatorial" planes are clearly seen. These planes pass through 5 atoms of the D_{5h}-modules tilted at an angle of 63.5° to the plane in which the axis of projection lies: the D_{5h}-modules at the ends of the diameters along C_5 axes (see Fig. 8, *a*) do not contact on the surface of the cluster and can be seen as "protrusions" on the surface of the 381-atom cluster, thus forming no fifth unbroken ring (see Fig. 8, *f*). These "protrusions" can also be seen on the projections of polyhedral models of the 381-atom cluster (see Fig. 8, *d*, *e*). Obviously, a cluster without these "protrusions," with more completed surface layer, and incomplete $\bar{1}(m\bar{1})_1$ *m* algorithm will be more stable. Since six out of the seven vertices of the D_{5h}-modules at the ends of diameters are unshared, the total number of atoms in the more stable cluster with the $\bar{1}(m\bar{1})m$ radial algorithm is $381 - 12 \cdot (7 - 1) = 309$.

471-Atom icosahedral cluster with mixed irregular algorithm $\bar{1}(m\ m\bar{1}m)$. A large 471-atom cluster[13] can be formed by using a mixed irregular radial algorithm $\bar{1}(m\ m\bar{1}m)$. Applying this algorithm along the diameter coinciding with the C_5 axis results in the formation of rods of three 55-atom Mackay icosahedra with radial algorithm $\bar{1}(m)_1$ along all C_5 axes. These rods interpenetrate to a depth of the common D_{5h}-module:

$$|_{D_{5h}}m_{D_{5h}}\bar{1}_{D_{5h}}m_{D_{5h}}[m_{D_{5h}}\bar{1}_{D_{5h}}m]_{D_{5h}}m_{D_{5h}}\bar{1}_{D_{5h}}m_{D_{5h}}|.$$

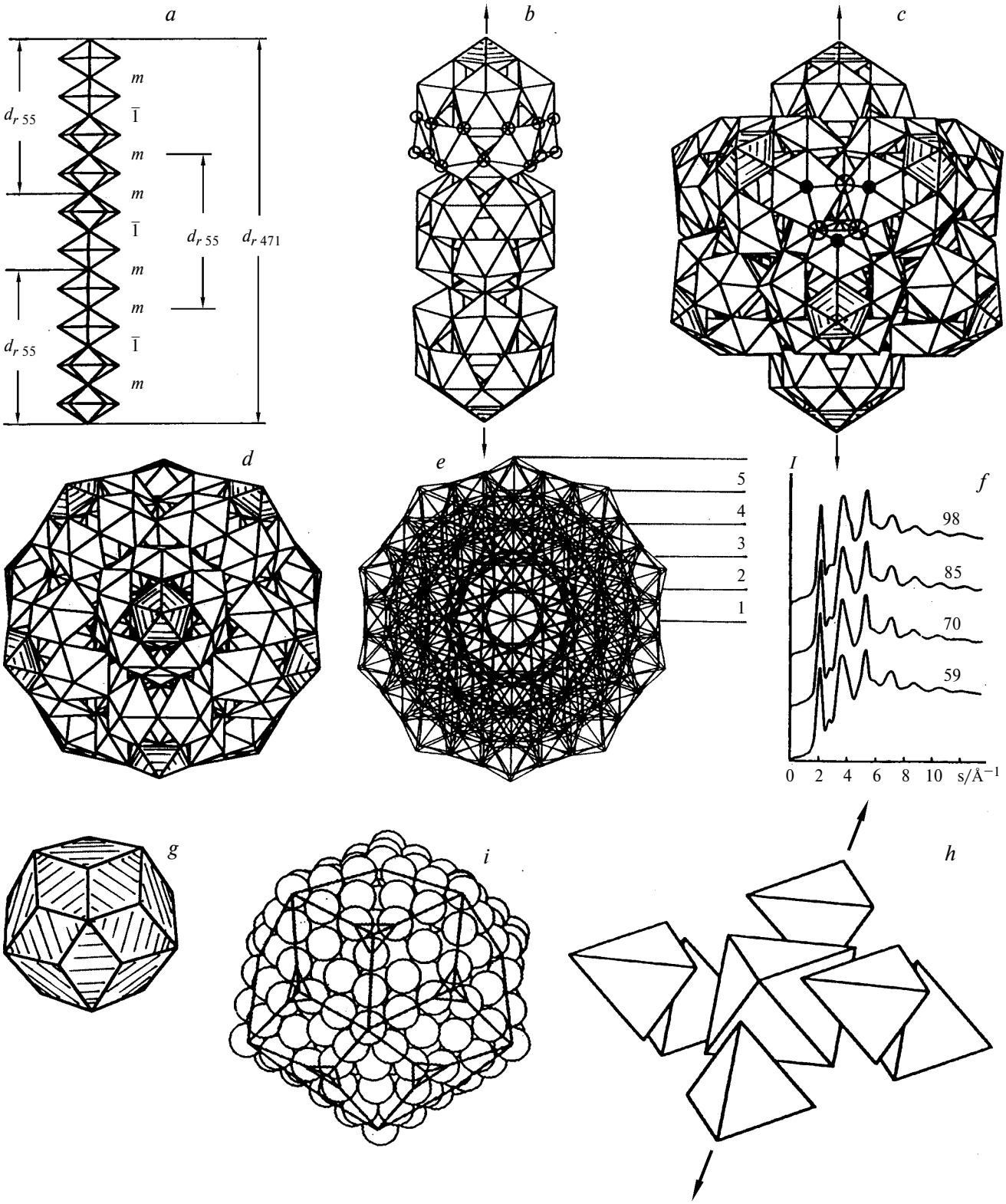

Fig. 9. Structure of the 471-atom icosahedral cluster with radial algorithm $\bar{1}(m\ m\bar{1}m)$: the chain of D_{5h}-modules along one of the C_5 axes in this module (*a*); the rod of three interpenetrating, 55-atom Mackay icosahedra along the C_5 axis (*b*); the 471-atom cluster (*c*) in the projection with the C_5 axis parallel to the drawing plane (the axis is shown by arrows); the 471-atom cluster in the setting along the C_5 axis (*d*); projections of all bonds along the C_5 axes (*e*, *h*) in the structure of the 471-atom cluster with triacontahedral habitus (*g*); the decagonal zone of the faces perpendicular to the drawing plane in the triacontahedron in the setting along the C_5 axis (*g*, *h*); electron diffraction patterns of clusters derived from the Mackay icosahedra[3] (*f*); and triacontahedral habitus of the 471-atom cluster[13] (*i*).

The "block diagram" of this full algorithm, as well as the structural fragments of the 471-atom cluster (a chain of ten D_{5h}-modules and a rod or three interpenetrating Mackay icosahedra), are shown in Fig. 9, *a* and *b*, respectively. The full algorithms of the Mackay clusters are shown by the lines and square brackets. Six of these rods along the diameters parallel to C_5 axes form a 471-atom cluster with triacontahedral morphology and small icosahedral faces formed by three atoms shown by filled circles in Fig. 9, *c* and taking off the edges of vertices on C_3 axes. The D_{5h}-modules at the ends of the rods of the Mackay icosahedra on the C_5 axes of the 471-atom cluster are hatched (see Fig. 9, *c*). One of these six rods lies in the drawing plane. The triacontahedral habitus of the 471-atom cluster[13] shown in Fig. 9, *i* can also be clearly seen if the polyhedral representation of this cluster is projected along the C_5 axis. The traces of ten faces perpendicular to the drawing plane are clearly seen on the contour of this cluster projection (Fig. 9, *d*—*h*). The triacontahedron is a zonohedron, therefore ten of its faces form a prism with the edges parallel to C_5 axes, which can be seen on the projection along the C_5 axis (see Fig. 9, *g*).

The number of atoms in the cluster can be calculated using the full notation of its algorithm. Twelve Mackay icosahedra joined to the central Mackay icosahedron on all C_5 axes (taking into account shared 7-atom D_{5h}-modules) form a cluster with $55 + (55 - 7) \cdot 12 = 55 + 576 = 631$ atom (without other shared vertices). Each of the 12 added Mackay clusters contacts its neighbors, so that 20 atoms on the surface of each Mackay icosahedron are simultaneously shared with another two such icosahedra. These atoms are shown as circles in Fig. 9, *b*, *c*. Thus, one should subtract 2/3 of the total number of shared vertices from the total number of atoms (631) in the cluster with the $\bar{1}(m\ m\bar{1}m)$ radial algorithm, $N = 631 - (2/3)(12 \cdot 20) = 471$. The peculiarities of external and "internal" morphology can also be recognized from the projection of all bonds in the structure of the 471-atom cluster along the C_5 axis (see Fig. 9, *e*, *h*). A system of five equidistant rings separated by an average distance of 2.32 Å (R(M—M)sin 63.5° = 2.6 Å · 0.895 = 2.32 Å) is also clearly seen. Thus, most of the atoms in all icosahedral clusters, irrespective of their radial algorithms, are in the layers of shells of different thickness embedded in each other as equidistant spheres, the number of which is equal to the total number of D_{5h}-modules in the full radial cluster algorithms. The number of D_{5h}-modules in the radial algorithm determines the diameter of the icosahedral clusters along the C_5 axis. Therefore, a system of equidistant maxima must be observed on the radial distribution curves of icosahedral clusters obtained by diffraction methods. Moreover, an analogous system of equidistant maxima will also be observed on the radial distribution curves of the clusters with one or several incomplete "icosahedral" outer shells. A system of equidistant diffraction maxima on the electron diffraction patterns of the 59-, 70-, 85-, and 98-atom clusters[3] based on the structure of the Mackay cluster and the 127-atom cluster with the $\bar{1}(m\bar{1})$ radial algorithm and two incomplete outer shells is shown in Fig. 9, *f*.

Using the projection of the bonds of the 471-atom cluster, one can reconstruct the motif of D_{5h}-modules on the outer surface of the cluster (see Fig. 9, *h*). The reconstructed modular network on the cluster surface and the system of cluster edges (see Fig. 9, *d*) shown by solid lines correspond to the projections of this cluster in the modular (see Fig. 9, *h*) and atomic (see Fig. 9, *i*)[13] representation.

The following rule is valid for the clusters with the same number of D_{5h}-modules in radial algorithms: the larger the number of binary symmetry operations *m* corresponding to the unstrained and less distorted Euclidean layers in the cluster algorithm, the larger the number of atoms in the cluster. Among icosahedral clusters with five D_{5h}-modules in the radial algorithms, the largest number of atoms (561) has the cluster of the Chini series with the $\bar{1}(m)_4$ radial algorithm. The cluster with three binary symmetry operations *m* in the radial algorithm, $\bar{1}(m\ m\bar{1}m)$, has a smaller number of atoms (471) and the cluster with two binary symmetry operations *m* in the radial algorithm, $\bar{1}(m\bar{1})_2$, has only 381 atom.

Conclusion

We also analyzed some analogies between the structures of the icosahedral metal clusters and fullerenes in the context of modular design. Let us outline in brief the parametric relationships between the structures of these clusters and fullerenes of the types I and II.[35] The objectivity of the existence of such relationships is confirmed by the fact that the classification of two-dimensional spherical structures with icosahedral symmetry by different P-classes* is based on the difference in orientation of their atomic nets with respect to the planar layer of the fcc close packing.[48] This classification was used for systematization of the capsules of various viruses, which are giant two-dimensional spherical clusters of protein globules.[49] The models of these capsules were constructed on the basis of the fractal structures of bound water in which the globules are located in their positions in giant, "twist-boat" type hexacycles of water rods with $p6_322$ symmetry due to the formation of multiple hydrogen bonds.[33]

In contrast to the three-dimensional structures of icosahedral clusters with several binary symmetry operations $\bar{1}$ in the radial algorithms, a two-dimensional icosahedral shell can be embedded in the three-dimensional Euclidean space with no restrictions imposed on

* The concept of P-class is generally accepted for description of the structures of icosahedral viruses.[48] The numbers in the notations of P-classes correspond to the periods of the edges of icosahedral clusters between two C_5 axes, expressed in units of the primitive lattice constant of hexagonal close packing.

its size.[50] Atomic arrays of the shells of fullerenes of the type I (the P3 class) commensurately coincide with the arrays of the close-packing layer, which forms spherical shells of the P1 class. Therefore, ignoring the rounding of the edges, the shells of icosahedral fullerenes of the type I can be considered as analogs of the particular layers of the Chini icosahedral metal clusters with radial algorithms $\bar{1}(m)_p$, which have another type of two-dimensional modules (hexagons instead of rhombi).

The compatibility of the layer metrics and, hence, the parameters of the shells of the layers based on the fcc packing and the graphite-like nets is evident. If a doubly base-centered H-cell[51] is chosen instead of primitive hexagonal P-cell in a close-packed layer of spheres, then, in the H-cell, the atoms of a graphite-like net are ordered and occupy 2/3 of the positions in the net of the close packing layer. Therefore, it is natural that the number of carbon atoms in icosahedral fullerenes of the type I is equal to 2/3 of the total number of atoms (N_n) in the layers of icosahedral metal clusters ($N_n = 10n^2 + 2$,[34] where $n = 3m$, n is the number of the layer in the Chini metal cluster, and m is the number in the series of fullerenes of the type I). The smallest fullerene of the type I, C_{60} ($m = 1$), is a "derived" analog of the third layer of the Chini 147-atom icosahedral metal cluster ($2/3 \cdot 10 \cdot 3^2 = 60$), the next "homologue" of this series (C_{240}) is a derivative of the sixth layer of the 923-atom cluster ($2/3 \cdot 10 \cdot 6^2 = 240$), *etc*. In fullerenes of the types I and II (the P3 and $P\sqrt{3}$ classes), the orientations of the layers of their shells with respect to the net of the close packing layer (the P1 class) are such that the surface area of the triangular "face"* of the type I fullerene (the P3 class) is three times larger than that of the "face" of the type II fullerene (the $P\sqrt{3}$ class). Hence, judging from the same value of the packing coefficient of the atoms in the shells of both fullerene types, the number of atoms in the type I fullerenes (N_I) must be three times larger than that in the type II fullerene shells (N_{II}) for the same value of the parameter K, which corresponds to the number of periods along their edges. Empirical parametric relationships $N_I = 60K^2$ and $N_{II} = 20K^2$ have been reported[35] without geometric substantiation.

Analogies between the structure of fullerenes and icosahedral metal clusters of the Chini series with the $\bar{1}(m)_p$ radial algorithm are confirmed by the existence of two types of multilayer spherical fullerene structures, a) icosahedral hyperfullerenes of the types I and II formed by two or three shells of icosahedral fullerenes embedded in each other[35] and b) spherical "onion" structures consisting of 15 and more shells.[52] Similar spherical layers equidistantly embedded in each other are observed for all icosahedral metal clusters (see Fig. 7, *h*, *j*; Fig. 8, *f*; and Fig. 9, *e*). As in the icosahedral metal clusters, the external shells in the "onion" carbon structures are strained, whereas the internal shells are compressed. Therefore, these "onion" structures are like nanoscopic spherical high-pressure chambers of diameter 35 to 40 nm. Irradiation of these structures with an electron beam leads to the formation of diamond nanocrystals of size up to 10 nm at the center of the chambers at 730 °C.[52]

Apart from carbon, the fullerene-like and spherical "onion" structures are formed by MoS_2 and WS_2. These compounds have a layered structure[53—55] in which the metal and sulfur atoms form nets similar to the close-packed layers.[15]

Eventually, the existence of the $C_{60}Ca_x^+$ clusters (x = 32; 104; 236; 448)[35] in which the multilayer icosahedral clusters of Ca atoms are formed on fullerene C_{60} used as a "seed," also confirms the existence of structural analogy between the icosahedral metal clusters and fullerenes as well as their parametric relationship.

The application of modular design appeared to be efficient for creating previously unknown models of the structures of alkali metals and the metals, which crystallize in the hexagonal close packing.[6,10] The alkali-metal clusters are of interest, since the number of atoms in their structures correlates with the number of electrons in successively filled orbitals: $1s^2$ (2); $1s^21p^6$ (8); $1s^21p^61d^{10}2s^2$ (20), *etc*.

Yet another important feature of the design of the structures of related clusters is that, in contrast to the fcc structure, in the bcc and hcp structures twinning along the most densely packed layers ({110} and {0001}) that are the faces of their simplices and modules is impossible.[56] Therefore, in this case we had to search for new possibilities for twinning of modules and simplices as the main binary symmetry operation that disturbs periodicity but retains the local order. On the one hand, this gave rise to additional difficulties; on the other hand, a much smaller number of feasible variants of symmetry modular design of the structures of these clusters compared to the clusters of the atoms of fcc metals was left. Determinism of the results obtained using the principles of modular design is confirmed by their systemic coincidence with experimental data and by consistency with the "jellium" model of the electronic structure of clusters.[6,10]

The modular design that appeared to be rather fruitful in the case of icosahedral metal clusters was then applied by the authors to the modeling of structures of smaller metal clusters with local orders of the hexagonal close and body-centered cubic packings.

* At the vertices of the "faces" of fullerenes of the types I and II are pentacycles corresponding to the outcomes of C_5 axes in the shells of their structures.

References

1. D. J. Wales, M. A. Miller, and T. R. Walsh, *Nature*, 1998, **394**, 758.
2. J. S. Bradley, in *Clusters and Colloids (From Theory to Applications)*, Ed. G. Schmid, VCH, Weinheim, 1994, 459.

3. P. H. Gaskell, in *Topics in Applied Physics*, *Glassy Metals II*, Eds. H. Beck and H.-J. Guntherodt, Springer-Verlag, Berlin, 1983, **53**, 5.
4. J. Friedel, *J. de Phys., Coll. C2, Suppl.*, 1977, **38**, C2-1.
5. Phan Van An and N. A. Bulienkov, *Mat. Sci. Research Int.*, 2000, **6**, 28.
6. N. Rösch and G. Pacchioni, in *Clusters and Colloids (From Theory to Applications)*, Ed. G. Schmid, VCH, Weinheim, 1994, 5.
7. N. N. Medvedev, *Metod Voronogo—Delone v issledovanii structury nekristallicheskikh sistem* [*Method of Voronoi—Delone in the Studies of the Structure of Non-Crystalline Systems*], Izd. Sib. Otd. RAN, Novosibirsk, 2000, 209 pp. (in Russian).
8. N. A. Bulienkov, in *Vestnik Nizhegorod. Un-ta im. N. I. Lobachevskogo, Ser. Fizika tv. tela* [*Nizhny Novgorod Univ. Bull., Solid State Physics Ser.*], 1998, Iss. 1, 19 (in Russian).
9. A. L. Makkei, in *Strukturnye issledovaniya kristallov* [*Studies on Crystal Structure*], Nauka, Moscow, 1996, 430 (in Russian).
10. W. A. de Heer, *Rev. Modern Phys.*, 1993, **65**, 612.
11. M. Schmidt, R. Kusche, B. von Issendorf, and H. Haberland, *Nature*, 1998, **393**, 238.
12. G. Bertsch, *Science*, 1997, **277**, 1619.
13. J. A. Barker, *J. de Phys., Coll. C2, Suppl.*, 1977, **38**, C2-37.
14. R. V. Galiulin, *Kristallograficheskaya geometriya* [*Crystallographic Geometry*], Nauka, Moscow, 1984, 134 pp. (in Russian).
15. N. V. Belov, *Struktura ionnykh kristallov i metallicheskikh faz* [*Structure of Ionic Crystals and Metal Phases*], Izd. AN SSSR, Moscow, 1947, 236 pp. (in Russian).
16. N. A. Bulienkov, in *Quasicrystals and Discrete Geometry*. The Fields Inst. Monogr., Ed. J. Patera, Am. Mathem. Soc., Providence (RI), 1998, **10**, 67.
17. E. S. Fedorov, *Simmetriya i struktura kristallov* [*Symmetry and Crystal Structure*], Izd. AN SSSR, Moscow—Leningrad, 1949, 630 pp. (in Russian).
18. D. Zhang and R. G. Cooks, *Int. J. of Mass Spectrometry*, 2000, **195/196**, 667.
19. N. A. Bulienkov, *Dokl. Akad. Nauk SSSR*, 1985, **284**, 1392 [*Dokl. Chem.*, 1985 (Engl. Transl.)].
20. J. D. Bernal, *Kristallografiya*, 1962, **7**, 507 [*Sov. Phys.-Crystallogr.*, 1962, **7** (Engl. Transl.)].
21. J. D. Bernal and S. H. Carlyle, *Kristallografiya*, 1968, **13**, 927 [*Sov. Phys.-Crystallogr.*, 1968, **13** (Engl. Transl.)].
22. A. L. Mackay, in *Symmetry: Unifying Human Understanding*, Ed. J. Hargittai, Pergamon Press, New York, 1986, 21.
23. N. A. Bulienkov, *Kristallografiya*, 1988, **33**, 422 [*Sov. Phys.-Crystallogr.*, 1988, **33** (Engl. Transl.)].
24. N. A. Bulienkov, *Kristallografiya*, 1990, **35**, 147 [*Sov. Phys.-Crystallogr.*, 1990, **35** (Engl. Transl.)].
25. N. A. Bulienkov, *Tez. dokl. II s'ezda biofizikov Rossii* [*Abstrs. IInd Russ. Biophys. Meeting*] *(Moscow, August 23—27, 1999)*, Moscow, 1999, **3**, 761 (in Russian).
26. N. A. Bulienkov, *Biofizika*, 1991, **36**, 181 [*Biophysics*, 1991, **36** (Engl. Transl.)].
27. J.-M. Lehn, *Supramolecular Chemistry, Concepts and Perspectives*, VCH, Weinheim—New York—Basel—Cambridge—Tokyo, 1995.
28. N. A. Bulienkov and Phan Van An, *CD-Proc. 12th Int. Conf. on Composite Materials (Paris, July 5—9, 1999)*, Paris, 1999, 1.
29. N. A. Bulienkov, *Dokl. Akad. Nauk SSSR*, 1986, **290**, 605 [*Dokl. Chem.*, 1986 (Engl. Transl.)].
30. Yu. A. Osip'yan, V. D. Negrii, and N. A. Bulienkov, *Izv. Akad. Nauk SSSR, Ser. Fiz.*, 1987, **51**, 1458 [*Bull. Acad. Sci. USSR, Phys. Ser.*, 1987, **51** (Engl. Transl.)].
31. G. Schmid, in *Clusters and Colloids (From Theory to Applications)*, Ed. G. Schmid, VCH, Weinheim, 1994, 1.
32. N. A. Bulienkov and V. S. Kraposhin, *Pis'ma Zh. Teor. Eksp. Fiz.*, 1993, **19**, 1 [*JETP Lett.*, 1993, **19** (Engl. Transl.)].
33. N. A. Bulienkov, *Kristallografiya*, 1990, **31**, 155 [*Sov. Phys.-Crystallogr.*, 1990, **31** (Engl. Transl.)].
34. B. K. Teo and N. J. A. Sloane, *Inorg. Chem.*, 1985, **24**, 4545.
35. T. P. Martin, *Phys. Rep.*, 1996, **273**, 199.
36. V. A. Engel'gardt, *Poznanie yavlenii zhizni* [*Cognition of Life Phenomena*], Nauka, Moscow, 1985, 303 pp. (in Russian).
37. L. Pauling, *The Nature of the Chemical Bond*, Cornell Univ. Press, Ithaca—New York, 1939.
38. B. K. Teo, H. Dang, C. F. Campana, and H. Zhang, *Polyhedron*, 1998, **17**, 617.
39. B. K. Teo and H. Zhang, *Inorg. Chem.*, 1991, **30**, 3115.
40. B. K. Teo, X. Shi, and H. Zhang, *J. Chem. Soc., Chem. Commun.*, 1992, 1195.
41. P. H. Gaskell, *Phil. Mag.*, 1975, **32**, 211.
42. A. L. Mackay, *Acta Crystallogr.*, 1962, **15**, 916.
43. V. L. Indenbom, N. V. Belov, and N. N. Neronova, *Kristallografiya*, 1960, **5**, 496 [*Sov. Phys.-Crystallogr.*, 1960, **5** (Engl. Transl.)].
44. N. Doraiswammy and L. L. Marks, *Phil. Mag.*, 1995, **B71**, 291.
45. B. E. Williams, H. S. Kong, and J. T. Glass, *J. Mat. Res.*, 1990, **5**, 801.
46. R. V. Galiulin, *Kristallografiya*, 1998, **43**, 366 [*Crystallogr. Repts.*, 1998, **43** (Engl. Transl.)].
47. H. S. Coxeter, *Regular Complex Polytopes*, Cambridge University Press, London, 1974.
48. B. K. Vainshtein, V. M. Fridkin, and V. L. Indenbom, *Sovremennaya kristallografiya* [*Modern Crystallography*], Nauka, Moscow, 1979, **2**, 359 pp. (in Russian).
49. D. L. D. Caspar and A. Klug, *Cold Spring Harbor Symp. Quant. Biol.*, 1962, **27**, 11.
50. H. S. M. Coxeter, *Introduction to Geometry*, J. Wiley and Sons, Inc., New York—London, 1961.
51. N. V. Belov, *Kristallografiya*, 1954, **4**, 268 [*Sov. Phys.-Crystallogr.*, 1954, **4** (Engl. Transl.)].
52. F. Banhart and P. M. Ajayan, *Nature*, 1996, **382**, 433.
53. R. Tenne, L. Margulis, M. Genu, and G. Hodes, *Nature*, 1992, **310**, 444.
54. R. Tenne, *Adv. Mater.*, 1995, **7**, 965.
55. P. A. Parilla, A. C. Dillon, K. M. Jones, and D. L. Schultz, *Nature*, 1999, **397**, 114.
56. M. V. Klassen-Neklyudova, *Mekhanicheskoe dvoinikovanie kristallov* [*Mechanical Twinning of Crystals*], Izd. AN SSSR, Moscow, 1960, 259 pp. (in Russian).

Received August 30, 2000